3

Sucrose, Sucralose and Fructose: Correlations Between Hydrophobicity Potential Profiles and AH—B—X Assignments[1]

FRIEDER W. LICHTENTHALER & STEFAN IMMEL

Institut für Organische Chemie, Technische Hochschule Darmstadt, D-6100 Darmstadt, Germany

ABSTRACT

MOLCAD program-mediated calculations of the molecular electrostatic potential (MEP) and of the respective lipophilicity (hydrophobicity) potential (MLP) on the contact surfaces of sucrose, galacto-*sucrose, sucralose and fructose are represented in 16 colour-coded form. Most informative with respect to the placement of the tripartite AH—B—X glucophore are the hydrophobicity distributions, which show the lipophilic X-part to be an entire, obviously quite flexible region rather than a specific corner of the 'sweetness triangle': in sucrose and sucralose encompassing the outside area of the fructofuranose moiety, in fructose the 1- and 6-CH_2 groups in either linked or separated form. In contrast, the hydrophilic portions of these sweeteners are more compact, invariably located opposite to the hydrophobic region, and appear to contain the AH—B couple of the glucophore: the glucosyl-2- and 3-OH group in sucrose and sucralose, versus the 3,4-diol grouping in fructose. Whilst absolute proof for these assignments is still lacking, support for their relevance is derived from the sweetness of altogether 53 sucrose derivatives and some fructose analogues. Most remarkably, the MLP profiles generated for the solid state conformations of some non-carbohydrate high-potency sweeteners, such as the sulfamides cyclamate, saccharin, and acesulfame, as well as structurally distinctly different dipeptides, e.g. aspartame, exhibit a hydrophobicity distribution strikingly similar to those observed for the sugars: hydrophilic and hydrophobic areas on opposite sites of the molecule. The results, particularly the MLP patterns*

presented, sustain the notion, that the sweet receptor with its proteinaceous 'hydrophobic cleft' — be it the same for sucrose, fructose, and non-carbohydrate sweeteners or different ones — is quite flexible in adapting to the complementary hydrophobic region of the sweet substance; following this 'docking procedure', the hydrophilic AH—B area of the substrate now being in its proper position, the sweet response is elicited via hydrogen bonding to a complementary receptor-based AH—B couple.

INTRODUCTION

The classical attempt by Shallenberger[2] and Kier[3] to rationalize the sweet taste of organic compounds presumes the existence of a common AH—B—X glucophore in all sweet substances, eliciting the sweet response via the interaction with a complementary tripartite AH—B—X site in the taste bud receptor.[4]

At the present state of our knowledge, however, this theory, also termed the 'sweetness triangle', appears much too simple to explain all of the observations, particularly when bearing in mind, that sweet-taste perception is mediated by a cascade of complex biochemical processes[5,6] that are little understood at the cellular and molecular level.

Nevertheless, the tripartite AH—B—X glucophore concept has had its merits as a unifying criterion and proved useful — despite its neglect of three-dimensional shape and volume — in rationalizing structure–sweetness relationships in such diverse classes of compounds as amino acids, dipeptides, sulfamides (e.g. saccharin and acesulfame), and sugars in particular, most notably the natural sweeteners sucrose (**1**) and fructose (**2**), as well as sucralose (**3**), a sucrose-derived high-potency sweetener. The availability of advanced computer modelling techniques, their application to the elucidation of the individual conformations of carbohydrates

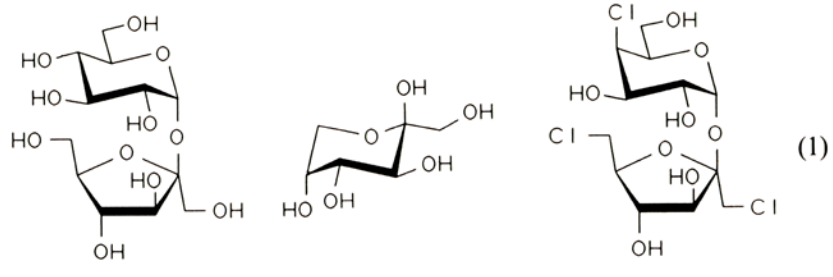

(1)

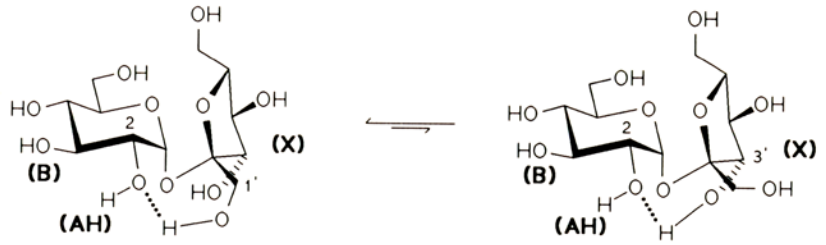

Fig. 1. Location of the tripartite AH—B—X glucophore in sucrose emerging from the computer-generated molecular electrostatic potential (MEP) and hydrophobicity potential (MLP) profiles.[8,9]

in vacuum and in solution,[7] particularly the possibility of representing various properties on the contact surface of sugars[8,9] have added a new dimension to the visual perception of sugars. Accordingly, not only may the electropositive and electronegative areas on the surface of a sugar molecule be reliably determined by computational methods, but the hydrophilic and hydrophobic regions as well,[8,9] which in terms of interactions with the sweet-taste receptor are apt to be of great significance.

Incorporation of such results into structure–sweetness considerations led us to a new allocation of the Shallenberger–Kier[2,3] tripartite AH—B—X glucophore in sucrose for the two forms likely to prevail in solution: the glucosyl-2-OH being the H-donor in this hydrogen bond interaction with a complementary acceptor group in the receptor, entailing the glucosyl-3-OH as the H-acceptor (B site), whilst the hydrophobic (lipophilic) X-part is an area on the 'outside' of the fructose moiety (Fig. 1).

Whilst these conclusions derived from the contact surface distribution of the molecular electrostatic potential (MEP) and the molecular lipophilicity (hydrophobicity) potential (MLP) of sucrose appear to be reasonable, they differ from alternate AH—B—X assignments as in Fig. 2, which are based on rationalizations of the sweetness of a sizeable number of sucrose analogues; as indicated in Fig. 2, the hydrophobic centre X is placed at the axial 4-position of the glucose moiety, because of the lack of sweetness of *galacto*-sucrose (the 4-epimer of sucrose), the sweetness of 4-deoxy-sucrose (1 ×) and the enhanced sweetness of 4-chloro-4-deoxy-*galacto*-sucrose (5 ×).[10–12] However, alternative hydrophobic centres had to be placed at the 1′- and 6′-positions of fructose to account for the increased sweetness (20 ×) of the respective 1′- and 6′-chloro-deoxy-sucroses.[10–12] In terms of the early suggestion of Shallenberger[14] that the presence of hydrophobic centres at different parts of the molecule may

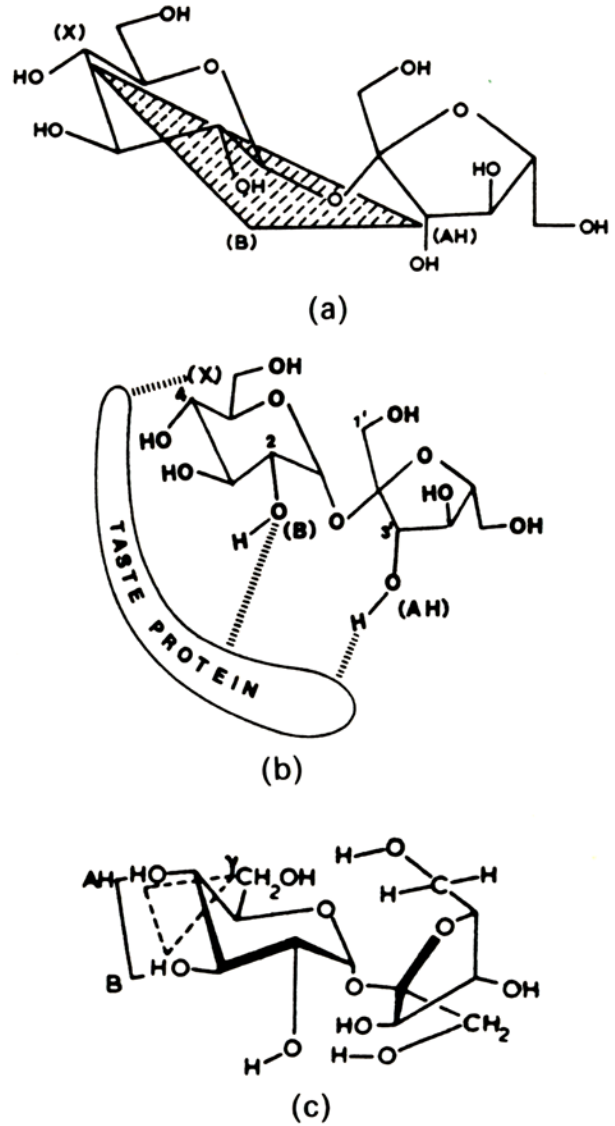

Fig. 2. AH—B—X glucophore assignments for sucrose as proposed by Hough *et al.* in 1989 (a[10] and b[11]) and by Mathlouthi *et al.* in 1990 (c[13]).

drastically disturb their orientation pattern, thereby preventing interactions of the AH—B units with the receptor site(s), multiple centres of hydrophobicity located in different portions of the sweetener appear to be unlikely.

In view of the fairly reliable MEP and MLP patterns on which the assignment in Fig. 1 is based, it appeared imperative to subject all sucrose derivatives of which the sweetness characteristics are known, to a thorough scrutiny with respect to the validity of the various AH—B—X assignments. This is done in the sequel based on the sweetness characteristics of deoxy-, *O*-methyl and deoxy-halo derivatives of sucrose. In addition, the hydrophobicity potential profiles of fructose (**2**), in its β-pyranoid form, and some non-carbohydrate sweeteners are probed as to their implications for the AH—B—X concept.

THE ELECTROSTATIC AND HYDROPHOBICITY POTENTIAL PATTERNS OF SUCROSE

As evidenced by X-ray data,[15] the conformation of sucrose in the crystalline state is determined by two intramolecular hydrogen bonds, one between the primary 6′-OH of fructose to the pyranoid ring oxygen of glucose (1·89 Å, cf. Fig. 3A, and stick-ball model in Fig. 4A), the other one between the 1′-hydroxyl group and the 2-O of glucose (1·85 Å). In solution, however, particularly in water, it is unlikely that both of these hydrogen bonds are retained; indeed, elaborate NMR investigations[16–19] strongly attest to the disintegration of the weaker 5-O$^{g}\cdots$HO-6^{f} hydrogen bond by solvation; for a dimethyl sulfoxide solution a competitive equilibrium between forms B and C has been deduced,[18] with the former predominating, cf. Fig. 3.

Several calculations of the energy potential surface of sucrose[16,20,21] have provided additional indications concerning the relevance of forms B and C, including ours[22] using the PIMM-88 force field program.[23] In Fig. 4, the solid state conformation of sucrose (A) is set against its PIMM-generated, lowest energy conformation B, in which the remaining intramolecular hydrogen bond has been slightly widened to 2·00 Å. This conformation being a realistic model for sucrose in (aqueous) solution — and, hence, for the form entering into the receptor site — the contact surface[24] (roughly equivalent to the solvent-accessible surface,[25] i.e. 'how water sees the molecule') was calculated using the MOLCAD-program methodology;[26] as is clearly evident from the dotted contours in Fig. 4, the transition from

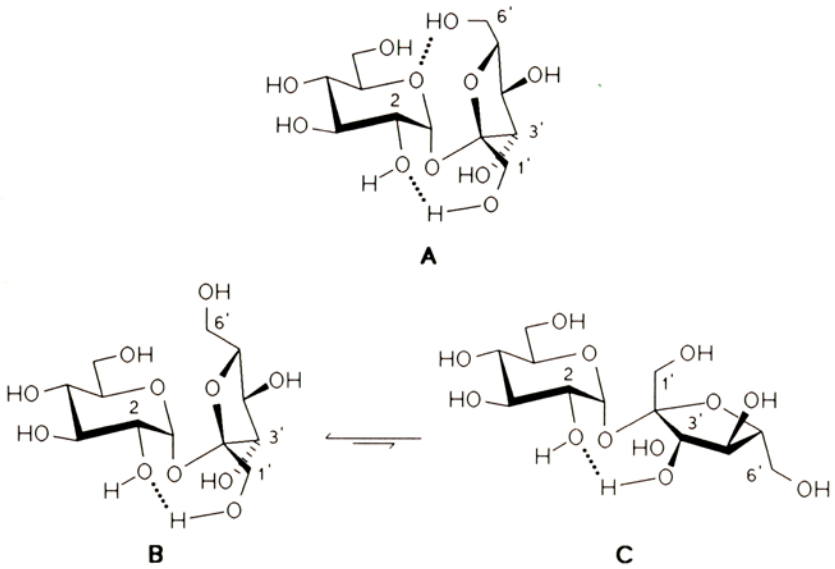

Fig. 3. Conformations of sucrose: (A) in the crystal as derived from neutron diffraction data;[15] for DMSO solution a competitive equilibrium B ⇌ C, with B predominating has been proposed.[18]

the solid state conformation (A) to that likely to be prevalent in solution (B) results only in minor changes on the 'upper' side of the molecule.

Calculations of the molecular electrostatic potentials[27] (MEP), i.e. the distribution of the charge density over the contact surfaces of the two sucrose conformations, were effected using the MOPAC[28] program-generated AM 1 atomic charges and have been represented in a 16 colour code ranging from violet (electropositive) to red (electronegative) (Plate 1). These reveal only minor differences in the overall electrostatic profile. As is clearly apparent from Plate 1, each of the forms has the violet, i.e. the most electropositive area centred around the glucosyl-2-OH, which in turn appears to be caused by the cooperative effect[29] of the intramolecular hydrogen bond directed towards this oxygen of this hydroxyl group. It may be noted, in this context, that an experimental verification of the validity of the MEP distribution of Plate 1 is provided by the behaviour of DMF solutions of sucrose under electrolysis conditions: the molecule is attracted to the cathode with its most electropositive, i.e. the glucosyl-2-OH portion, and, upon taking up an electron (to an alkoxyl radical anion) and releasing a hydrogen atom ($\rightarrow H_2$), leaves the glucosyl-2-oxygen

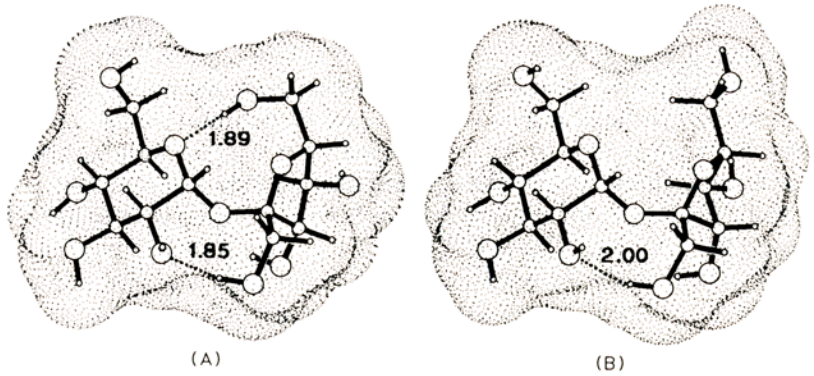

Fig. 4. Contact surface of sucrose (roughly equivalent to the solvent accessible surface) in dotted form with a stick-ball model insert, the larger balls representing oxygen atoms. (A): conformation in the crystal as derived from neutron diffraction data,[15] showing the two intramolecular hydrogen bonds 5-O^g · · · HO-6^f (1·89 Å) and 2-O^g · · · HO-1^f (1·85 Å). (B): lowest energy conformation emerging from PIMM-88 force field calculations[22] (for vacuum), lacking the 5-O^g · · · HO-6^f hydrogen bond.

deprotonated. This is evidenced by the fact that *in situ* alkylation or acylation (i.e. in the cathodic cell) produces the 2-*O*-substituted sucrose derivatives with high preference.[30]

The MEP pattern of sucrose as depicted in Plate 1 may thus be considered, with confidence, to properly represent the charge distribution in solution, and, accordingly, may be used to locate the AH—B part of the glucophore such that the AH-hydrogen is likely to be electropositive for interaction with an oppositely polarized binding site on the receptor; similarly, the inverse situation would have to prevail for the B portion. This reflection points towards the glucosyl-2-OH as the AH portion and the B part in its direct vicinity. However, it is seemingly unavailing to locate the hydrophobic X-site on the basis of the MEP pattern.

Since there is ample evidence to assume that the sweet-taste receptor is proteinaceous in nature, and that interaction between a hydrophobic portion on the protein surface with the corresponding hydrophobic portion of sucrose is involved in triggering the sweet-response, the reliable location of that is of major importance in structure-sweetness considerations. The recently advanced possibility to compute the molecular hydrophobicity (lipophilicity) potentials (MLP)[31] has been applied by us[8] to determine the MLP pattern for crystalline sucrose as depicted on the left

of Plate 2 in the same 16 colour code as used for the MEPs, violet representing here the most hydrophobic and red the respective hydrophilic areas. As is clearly evident from this representation, the hydrophilic and hydrophobic portions of the molecule are distinctly separated on opposite sides. Particularly clear is the half-opened form with the stick and ball-model insert, revealing the entire outside section of the fructose moiety to be hydrophobic (i.e. violet), and the hydrophilic red section to be centred around the 3-oxygen of glucose.[8]

Observation of the alternative sucrose conformation likely to prevail in solution (cf. Plate 2, right), reveals few changes in the overall MLP-pattern, except that the hydrophobic region located at the outer side of the fructose moiety is now more compact. In consequence, the part of sucrose able to engage in hydrophobic bonding within the sweet-taste receptor is to be assigned to an entire region of the fructose portion, rather than a specific position. In keeping with these notions, the location of the tripartite AH—B—X glucophore emerges in the form indicated in Fig. 1: the glucosyl-2-OH and -3-OH being the proton donor (AH) and proton acceptor (B) parts engaging in simultaneous hydrogen-bonding to a complementary (inverse) AH—B system on the receptor protein, whilst the hydrophobic X-part is a region centred around H-3 of fructose.

THE TRIPARTITE AH—B—X GLUCOPHORE IN SUCROSE DERIVATIVES

In securing corroborative evidence for the location of the AH—B—X glucophore, the sucrose derivatives considered are limited (for elimination of steric misfits) to those modified either by inversion, deoxygenation, and O-methylation of individual hydroxyl groups, or by their replacement with halogen.

The most direct method for probing into the location of the AH—B—X glucophore appears to be the replacement of a given hydroxyl group in sucrose by hydrogen and assessment of its effect on sweetness. As of now, however, sweetness data are available only for three of the eight mono-deoxy-sucroses, i.e. the 4-deoxy (**4**), 6-deoxy (**5**) and 1′-deoxy derivatives (**6**) (Table 1). All are less sweet than sucrose,[32,33] yet the fact that sweetness is not lost entirely may be taken as an indication that none of the hydroxyl groups removed (i.e. the 4-OH and 6-OH of glucose, and 1′-OH of fructose) occupy positions detrimental for eliciting the sweet response. Accordingly, the existence of the intramolecular 2-O^{g} ··· HO-1^{f} hydrogen

Table 1 Sweetness of 4-deoxy- (**4**), 6-deoxy- (**5**), and 1′-deoxy-sucrose (**6**).

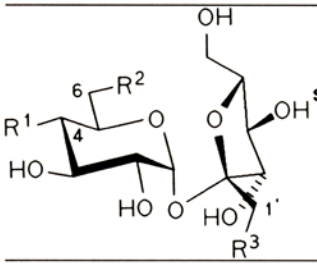

	R^1	R^2	R^3	*Sweetness*[a]	*Refs*
sucrose	OH	OH	OH	SS	—
4	H	OH	OH	S	32
5	OH	H	OH	S	32
6	OH	OH	H	S	32, 33, 35

[a] S = sweet and SS = very sweet.

bond in sucrose is obviously no prerequisite for proper interaction with the sweet receptor, a notion that is similarly emerging from the sweetness of 1′-*O*-methyl- and 1′-chloro-1′-deoxy derivatives of sucrose (cf. below). Unfortunately, sweetness data on the other five deoxy-sucroses (2- and 3-deoxy in particular) or any of the 28 possible dideoxy-sucroses, which would further contribute to this issue, are not yet available.

Next to deoxygenation, *O*-methylation of individual OH-groups in sucrose appears to be a suitable means of probing binding sites, provided that the steric expansion introduced by the OH → OMe conversion does not detract from the taste assessment. Such an impairment appears to be small, if at all, as evidenced by the data available for four mono- (**7**–**10**) and four dimethyl ethers of sucrose (**11**–**14**, Table 2):[32–35] any of the three primary OH-groups in sucrose may be *O*-methylated without losing sweetness, which also applies to the glucose-4-OH. In all of these methyl ethers

Table 2 Sweetness of methyl ethers of sucrose.

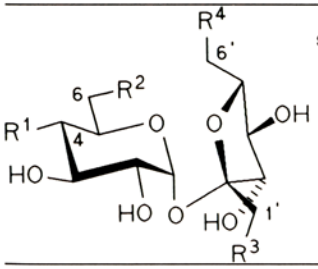

	R^1	R^2	R^3	R^4	*Sweetness*[a]	*Refs*
sucrose	OH	OH	OH	OH	SS	—
7	OMe	OH	OH	OH	S	34
8	OH	OMe	OH	OH	SS	32
9	OH	OH	OMe	OH	SS	33, 35
10	OH	OH	OH	OMe	SS	34
11	OMe	OMe	OH	OH	S	34
12	OMe	OH	OH	OMe	S	34
13	OH	OMe	OH	OMe	SS	34
14	OH	OH	OMe	OMe	S	34

[a] S = sweet and SS = very sweet.

Table 3 Taste characteristics of sucrose derivatives modified in the glucose portion at C-6.

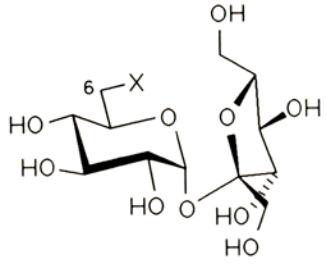

	X	Taste	Refs
sucrose	OH	sweet	—
5	H	sweet	32, 35
8	OMe	sweet	32, 35
15	OAc	slightly sweet	32, 35
16	OBn	bitter	32, 35
17	OBz	bitter	32, 35
18	OPO_3H	bitter	32, 35
19	Cl	bitter	32, 35, 36

the glucose-2- and -3-OH groups, i.e. the structural AH—B requirements of Fig. 1, remain untouched, thus their sweetness data may be taken as an affirmation of the glucophore assignment. Curiously, no sweetness data of sucrose derivatives methylated at O-2, O-3, or at both of these positions, which would shed further light on this issue, are available.

The 6-position in the glucose portion of sucrose appears to be a sensitive one with respect to the steric bulk introduced by its chemical modification. Whilst the 6-deoxy (**5**) and 6-*O*-methyl (**8**) derivatives are as sweet as sucrose, the 6-*O*-acetate (**15**) is only slightly sweet, the 6-benzyl ether (**16**), the 6-benzoate (**17**), and 6-phosphate (**18**) are bitter, as is the 6-chloro-6-deoxy compound (**19**, cf. Table 3). In the latter case, the obvious misfit introduced by the 6-chlorine substituent may be overcome by increasing the hydrophobicity of the fructose portion: 6′-chlorination (→ **20**) removes the bitterness; chlorination at both primary positions of the fructose portion result in a molecule (**21**) with enhanced sweetness (cf. Table 4).[10,35,36]

Configurational changes in the glucose portion of sucrose seem to have a more pronounced effect on the sweetness: its 4-epimer, the '*galacto*-sucrose' (**22**) has very low sweetness,[34] the 3-epimeric analogue, '*allo*-sucrose' (**23**), is tasteless.[37] This clearly indicates subtle stereochemical requirements for the substrate on entering and/or being embedded into the receptor site(s). In the case of the 3-epimer **23** this may be rationalized via the change of the steric requirements of the AH—B site, an axial 3-OH being incapable of properly functioning as the hydrogen bond-accepting B component.

That 3-*keto*-sucrose (**24**) is sweet[37] goes along well with the AH—B—X

Table 4 Taste characteristics of 6-chloro-6-deoxy-sucroses.

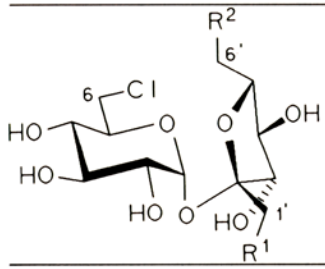

	R^1	R^2	Taste (sucrose sweetness = 1)	Refs
19	OH	OH	bitter	10, 35, 36
20	OH	Cl	not sweet	36
21	Cl	Cl	25	10, 35

tripartite glucophore assignment of Fig. 1, inasmuch as the 3-carbonyl function retains the hydrogen bond acceptor capabilities. Less well comprehensible is, at first sight, the very low sweetness of *galacto*-sucrose (**22**),[34] in which the 2-OH and 3-OH of the hexosyl portion, i.e. the AH—B site suggested in Fig. 1, is intact. A clue as to the possible reasons emerges from a comparison of the conformation of sucrose in solution, which features a *gg*-arrangement of the glucosyl-6-CH_2OH relative to the pyranoid ring (Fig. 5B), with the respective arrangements for its 4-epimer **22**. The PIMM-program generated, minimum energy conformations for **22** result in the forms depicted in Fig. 5 (B–D) which only differ by the orientation of the galactosyl-6-OH. Thereby, the *gg* form B, due to formation of a stabilizing intramolecular hydrogen bond 6-$OH^g \cdots O\text{-}4^g$, comes out to be about 4 and 8 kJ/mol more stable than the *tg*- (C) and *gt*-rotamers (D), yet it is clear that this only prevails *in vacuo*. For solution, there

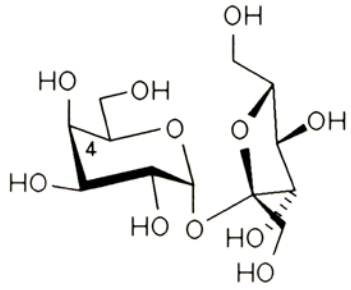

galacto-sucrose
22

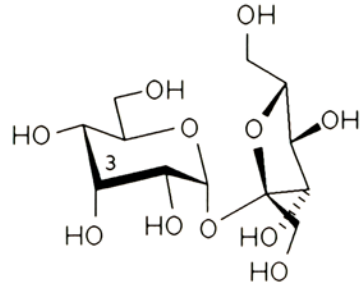

allo-sucrose
23

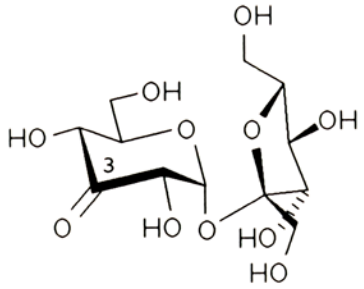

3-*keto*-sucrose

24

is abundant evidence in the literature,[38] that the sterically unfavourable 1,3-*syn*-interactions between 4- and 6-hydroxyl groups of a hexopyranose are evaded by solvation; hence, rotamers C and D of Fig. 5 will have to be entered into structure-sweetness considerations. Correspondingly, the sucrose conformation of Fig. 5A is to be set against those of *galacto*-sucrose depicted in Figs. 5(C, D): inversion of configuration at C-4 of sucrose entails a distinct change in the rotameric preference at the 6-OH, which is an *a priori* sterically sensitive position (*vide supra*, Table 3). Thus, the very low sweetness of *galacto*-sucrose may be taken as an indication that the C-6 substituent in the aldose portion of sucrose is not only sensitive towards steric bulk — any significant increase resulting in the loss of sweetness (cf. Table 3) — but also in its orientation to the pyranoid ring, with a *gg*-arrangement conceivably being favoured.

Another factor conceivably responsible for the substantial decrease in sweetness on inversion of the sucrose-4-OH may be found in the shift of the MLP pattern (Plate 3), of which the hydrophilic (red) area centred around C-3 of the glucose unit is shifted to the upper side as compared to sucrose in Fig. 4. That, on the other hand, 4-chloro-4-deoxy-*galacto*-sucrose exhibits a 5-fold higher sweetness than sucrose[36] can be attributed to the hydrophobic substituent at C-4, that changes the overall shape of the molecule and its MLP pattern substantially (as observed, for example, for the pyranoid portion of sucralose, cf. Plate 5).

Deoxy-halo-sucroses

Unlike the deoxy- and *O*-methyl-sucroses discussed so far, whose sweetness is of about the same or lower intensity than that of the parent sugar, some deoxy-halo derivatives of sucrose exhibit substantially enhanced

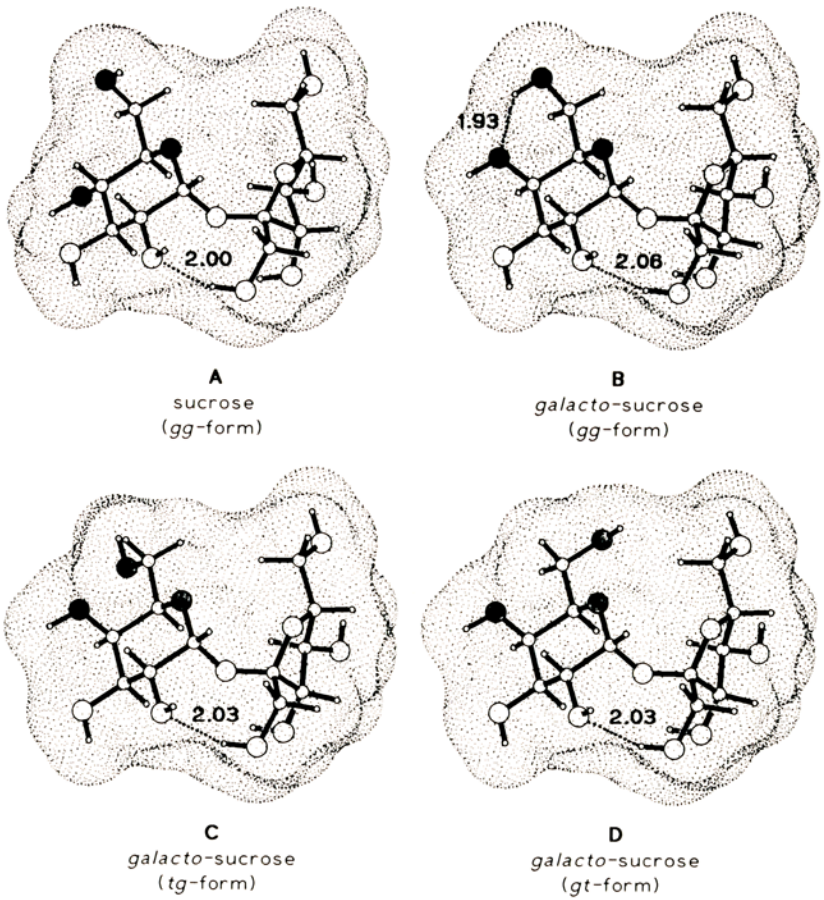

A
sucrose
(*gg*-form)

B
galacto-sucrose
(*gg*-form)

C
galacto-sucrose
(*tg*-form)

D
galacto-sucrose
(*gt*-form)

Fig. 5. Contact surface (in dotted form) of sucrose (A, featuring a *gauche-gauche* (*gg*) arrangement for the glucosyl-6-OH relative to the pyranoid ring) as compared to the three conformers of *galacto*-sucrose (**22**) generated by PIMM force field calculations: the *gg*-form B (in vacuum only), stabilized by an intramolecular hydrogen bond 6-OH^{9} · · · O-4^{9}, and the two forms relevant in solution, i.e. the *trans-gauche* (*tg*, C) and the *gauche-trans* (*gt*, D) rotamers. The oxygens involved in the designations and discussion (cf. text) are accentuated by filling.

Table 5 Relative sweetness of deoxy-halo-sucroses modified in the fructose portion.

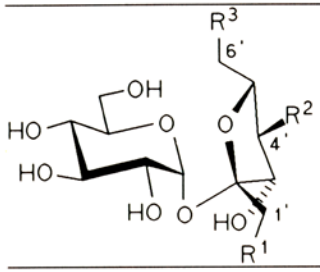

	R^1	R^2	R^3	Relative sweetness	Ref.
sucrose	OH	OH	OH	1	—
25	Cl	OH	OH	20	10, 35, 36, 45
26	OH	OH	Cl	20	10, 35, 36
27	Cl	Cl	OH	30[a]	46
28	Cl	OH	Cl	80	10, 35
29	Br	OH	Br	80	49
30	Cl	Cl	Cl	100	46

[a] In Table XIX on p. 266 of Lee's review[4] the relative sweetness for **27** is erroneously listed as being 3500.

sweetness, in specific instances even several thousand times that of sucrose. Following the discovery of the first compound of this type by Hough & Phadnis in 1976,[39] an impressively large number of deoxy-halo-sucroses have been synthesized and evaluated for their potency in sweet taste perception.[3,10–12,35,36,39–50] The total of 35 compounds listed in the following Tables provide a large body of experimental evidence that should be rationalizable in terms of the AH—B—X conceptual assignments made in Fig. 1.

The AH—B—X assignment of Fig. 1 implies that the hydrophobic cleft of the taste receptor protein corresponds to the hydrophobic region in the fructose moiety of sucrose (cf. Plate 2). In keeping with this notion, it may be predicted, that an increase of hydrophobicity in the fructose portion — i.e. along the violet portion in the MLP profile (Plate 2) — favours binding to the corresponding hydrophobic site in the receptor, and hence enhances sweetness. Indeed, the data collected for the compounds **25–30** (Table 5) support this rationalization, since replacement of the fructose hydroxyl groups at the 1′-, 4′-, and/or 6′-position by chlorine or bromine uniformly leads to compounds sweeter than sucrose.

Analysis of the sweetness characteristics of the numerous 4-halo-4-deoxy-*galacto*-sucroses (Table 6) in terms of the AH—B—X assignment of Fig. 1 is particularly informative. A shift of the substantially hydrophilic glucosyl-4-OH of sucrose (red area in Plate 2) from the equatorial to the axial orientation (→*galacto*-sucrose (**22**), cf. Plate 3), together with the accompanying change in the rotameric arrangement of the 6-OH[g] (cf. Fig. 5) results in a near loss of sweetness.[34] However, when placing a markedly

Table 6 Relative sweetness (sucrose = 1) of 4-deoxy-4-halo-*galacto*-sucroses.

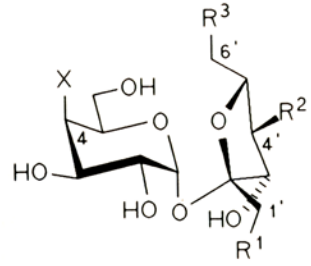

	Glucose X	Fructose R^1	R^2	R^3	Relative sweetness[a]	Refs
sucrose	OH	OH	OH	OH	1	—
31	Cl	OH	OH	OH	5	10, 36, 45
32	Cl	OH	OH	Cl	50	49
33	Cl	Cl	OH	OH	120	10, 35
34	Cl	OH	Cl	Cl	160	46
35	Cl	Cl	Cl	OH	220	46
3[b]	Cl	Cl	OH	Cl	650	43
36	Cl	Br	OH	Br	800	49
37	Cl	Cl	F	Cl	1000	46
38	Cl	Cl	Cl	Cl	2200	44, 47
39	Cl	Cl	Br	Cl	3000	46
40	Cl	Cl	I	Cl	3500	43, 46
41	Cl	Br	Br	Br	7000	46
42	F	OH	OH	F	4	49
43	F	F	OH	F	40	43
44	F	Cl	Cl	Cl	200	46
45	Br	Cl	OH	Cl	375	49
46	Br	Br	OH	Br	800	49
47	Br	Br	Br	Br	7500	43, 46
48	I	I	OH	I	120	43, 49

[a] All of these data were retrieved from the original literature as indicated by the respective references. It should be noted that a number of sweetness values given in Lee's review (*Adv. Carbohydr. Chem. Biochem.* **45** (1987). Table XIX on p. 266) are at error, most notably the data listed for compound **40** (7000 instead of 3500), and **41** (30 instead of 7000).
[b] Sucralose.

hydrophobic substituent such as chlorine into the very same axial position, the sweetness, relative to sucrose, is enhanced by a factor of 5 (compound **31** in Table 6).

The comparison of the sweetness of 4-chloro-4-deoxy-*galacto*-sucrose (**31**) with that of its analogues **32–41** is particularly instructive, inasmuch as the successive replacement of the fructose 1′-, 4′-, and 6′-OH groups translates into substantially increased sweetness values, the 1′,4′,6′-tribromo analog **41** featuring a 1400-fold enhancement over **31**. An essentially identical trend is observed in the two 4-deoxy-4-fluoro-*galacto*-sucroses **42** and **43** [a 10-fold increase of sweetness from the 4,6′-difluoro

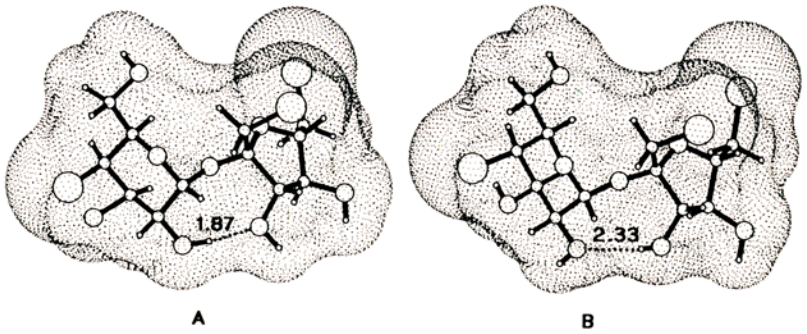

Fig. 6. Contact surface of sucralose (**3**) in dotted contours with a stick-ball model insert, the large balls representing the three chlorine atoms at position 4 of the hexose, and positions 1 and 6 of fructose: (A) conformation in the crystal as derived from X-ray data;[52] (B) lowest energy conformation emerging from PIMM force field calculations,[64] with an inverted intramolecular hydrogen bond 3-OH$^{f}\cdots$O-2^{g}, resembling more closely the conformation proved to prevail in solution.[53]

42 to the 4,1′,6′-trifluoro compound **43**], and very markedly, in the 4-bromo analogues **45–47**, in which the enhancement of sweetness perception reaches a solitary maximum.

Of these compounds in Table 6, sucralose (**3**), a non-caloric high-potency sweetener recently approved for food use,[51] was selected to further probe into the hydrophobic/hydrophilic portions of the molecule by computer modelling, an intent facilitated by the availability of its X-ray structure.[52] In Fig. 6 the molecular geometries and their contact surfaces are depicted for two forms of sucralose, Fig. 6A representing the crystalline state conformation based on X-ray data and Fig. 6B the state likely to prevail in solution,[53] as generated by force field optimizations. It is interesting to note, that the directionality of the intersaccharidic hydrogen bond is reversed on going from the crystal (A, 2-OH$^{g}\cdots$O-3^{f}) to the lowest energy, computer simulated form (B, 2-O$^{g}\cdots$HO-3^{f}).[64]

Portraying on this contact surface the MOLCAD-generated MEP-pattern, it is evident from Plate 4, that the form relevant for solution (closed and opened form on the right each), is as markedly electropositive (violet) as observed for sucrose (cf. Plate 1), obviously due to an analogous direction of the 2-O$^{g}\cdots$HO-3^{f} hydrogen bond.

The hydrophobicity potential profile pictured in Plate 5, expectedly shows the two chlorine atoms in the fructose portion to be the hydrophobic

Table 7 Relative sweetness (sucrose = 1) of sucralose (**3**) analogues.

		X	*Y*	*Z*	*Relative sweetness*	*Refs*
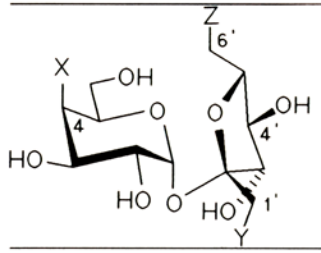	**43**	F	F	F	40	43
	3[a]	Cl	Cl	Cl	650	43
	36	Cl	Br	Br	800	49
	45	Br	Cl	Cl	375	49
	46	Br	Br	Br	800	49
	48	I	I	I	120	43, 49

[a] Sucralose.

centre (X-site), now being extended over the entire 'outside' region of fructose (as compared to sucrose, cf. Plate 2). Another obvious similarity with sucrose is the fact, that hydrophobic (violet) and hydrophilic (red) regions are located on opposite sides of the molecule, seemingly little disturbed by the third chlorine at the C-4 of the pyranoid ring, which — as is clearly evident from Plate 5 — is less hydrophobic than the other two.

An interesting relationship between sweetness and the nature of the halo substituent in sucralose analogues is revealed by the data listed in Table 7. Sucralose (4,1′,6′-trichloro-trideoxy-*galacto*-sucrose, **3**), is 16-fold sweeter than its trifluoro analog **43**, and approximately 5 times sweeter than the triiodo compound **48**, indicating that fluorine is too small and iodine is too big to properly fit into the receptor binding site(s). The best fit appears to be provided by bromo substituents in the fructose 1′- and 6′-positions, as evidenced by compounds **36** and **46**, which are 800 times sweeter than sucrose.[43,49]

Another probe into the effect of the 6-substituent on sweetness is provided by the sucralose analogues additionally substituted at C-6 (Table 8): in comparison to compound **3**, the sweetness of the 4,6,6′-trichloro isomer **49**, which lacks the sweetness enhancing 1′-chloro substituent in the hydrophobic centre of the fructose portion, drops dramatically (650 → 4), a decrease that is only partially made up by introducing the 1′-chloro group (4 → 200 for **50**), due to the presence of the critical 6-Cl substituent (cf. Table 3). As expected from the discussion of 6-deoxy- and 6-*O*-methyl-sucrose (Tables 1 and 2), modification of the 6-substituent by deoxygenation (→compound **51**) and O-methylation (→**52**) has only a

Table 8 Relative sweetness (sucrose = 1) of some 4,6′-dichloro substituted *galacto*-sucroses (analogues of sucralose **3**) modified at C-6.

		X	R^1	*Relative sweetness*	*Refs*
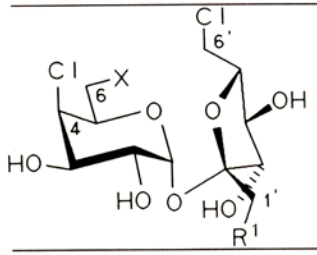	**3**[a]	OH	Cl	650	43
	49	Cl	OH	4	45
	50	Cl	Cl	200	45
	51	H	Cl	400	43, 48
	52	OMe	Cl	500	43, 48
	53	O*i*Pr	Cl	not sweet	43

[a] Sucralose.

minor effect on the intensity of the sweetness sensation. Yet, increase of the steric bulk at C-6 from OCH_3 (**52**) to $OCH(CH_3)_2$ (**53**) is seemingly fatal, as sweetness is lost completely.

Oddly enough, sucrose derivatives modified at either the glucosyl-2-OH or -3-OH group, like the deoxy-, *O*-methyl- or chloro-analogues, are not available. Sweetness data on these would have a major bearing on the AH—B assignment as in Fig. 1. The only examples along these lines are the two 2-chloro-2-deoxy-mannosyl analogues. The dichloride **54** has been found to be 'not sweet at all',[46,47] and the tetrachloride **55**, despite its additional hydrophobicity- and, hence, sweetness-enhancing 6′-chloro substituent, is 'as bitter as quinine'.[50]

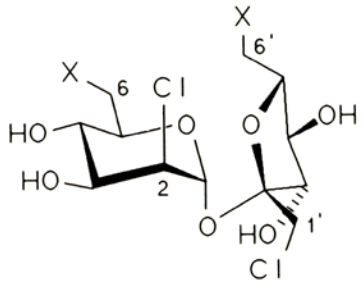

54 X = OH (not sweet at all)[46,47]

55 X = Cl (very bitter)[50]

This finding, along with the observation that *allo*-sucrose (**23**) is not sweet, emphasizes that there are strict steric requirements for the arrangement of the 2- and 3-hydroxyl groups, and that their equatorial orientation is seemingly essential for eliciting the sweet sensation. This conclusion is also in accord with, but not absolute proof of the AH—B assignments to the 2- and 3-OH groups of the glucosyl moiety in sucrose.

By way of summary, the foregoing discussion of the sweetness of over 50 derivatives or analogues of sucrose provides ample evidence for placing the hydrophobic X-site of the Shallenberger–Kier glucophore onto the outside region of the fructose portion rather than to other parts of the sucrose molecule. This is borne out by the MLP patterns presented, and by the fact that an increase of the hydrophobicity in the fructose portion invariably results in an enhancement of sweetness. In keeping with the notion that the X part is mainly responsible for orientation of the molecule in entering and/or being embedded into the receptor site, it can be assumed, that this hydrophobicity-controlled 'docking procedure' of the substrate into the hydrophobic cleft of the receptor is required for bringing the AH—B portions into the proper receptor positions to elicit the sweetness sensation via hydrogen bonding.

Placement of the hydrophobic X part into the fructose portion of sucrose leaves little alternative for the AH—B part: 4-deoxy- and 6-deoxy-sucrose are sweet, albeit less than sucrose (Table 1), as are the respective 4-*O*- and 6-*O*-methyl ethers (Table 2) — findings that render these positions most unlikely as those essential for eliciting the sweet response. In contrast, the data discussed above point towards the location of the AH—B unit in the diol grouping made up by the glucosyl-2-OH and -3-OH groups. Both are situated within the most hydrophilic region of sucrose (cf. Plate 2), and principally, each may be assigned the B (or AH) part. In our recent proposal the AH part was assigned to the glucosyl-2-OH, mainly for the reason that the MEP pattern of Plate 1 indicates this hydroxyl group to be the most electropositive, and hence, is conceivably better disposed to engaging its OH-proton as donor in a substrate-receptor hydrogen bond.

In toto, the evidence for the assignment of the AH—B—X glucophore, as depicted in Fig. 7, though not definitive, is a most useful working hypothesis for rationalizing sweetness data in sucrose derivatives, and surely worthy of further attention. We expect that greater certainty will come from the sweetness data of the five remaining deoxy-sucroses (particularly the 2- and 3-deoxy compounds), and of the four missing monomethyl ethers, especially the 2-*O*-methyl- and 3-*O*-methyl-sucroses. Other desirable derivatives with which the validity of the assignments could be further probed, are 2-*epi*-sucrose, i.e. its mannosyl analogue, and its 3′-epimer, a *psico*-sucrose.

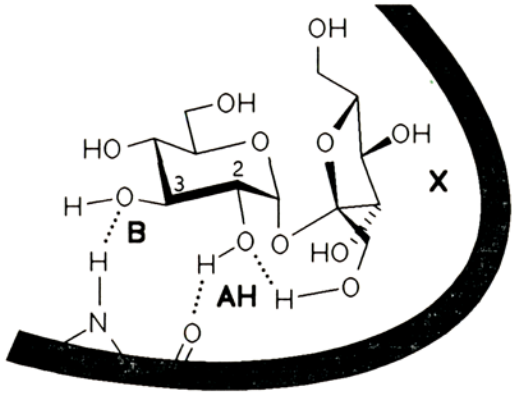

Fig. 7. Location of the tripartite AH—B—X glucophore ('sweetness triangle') in sucrose emerging from the computer-generated molecular electrostatic potential (MEP) and the molecular lipophilicity potential (MLP) profile.

β-D-FRUCTOPYRANOSE: CONFORMATIONS AND MLP PROFILES

D-Fructose crystallizes in the β-D-pyranoid form, as evidenced by X-ray structural data.[54] Freshly prepared solutions are almost twice as sweet as sucrose (1·8 ×),[55] but when equilibration of the β-*p*-form to the tautomeric β-*f*-, α-*f*-, and α-*p*-forms (cf. Fig. 8) is complete, the solution is only slightly sweeter than one of sucrose of equal w/v-concentration.[55] From this it was inferred that the two furanoid forms are either substantially less sweet than the β-*p*-form or devoid of sweet taste entirely, a conclusion that is supported by the parallelism of decrease of sweetness and of β-*p*-form (in the equilibrium tautomeric mixture) on increasing the temperature.

By consequence, fructose-sweetness considerations are all based on the β-*p*-form, and several assignments for the tripartite AH—B—X glucophore have been advanced: (i) Shallenberger *et al.*[58] intuitively, and Lindley & Birch,[59] on the basis of consideration of model compounds,[59] arrived at the anomeric 2-hydroxyl group and the hydroxymethyl oxygen as the AH—B couple, respectively (Fig. 9 (i)). The inverse assignment (Fig. 9 (ii)) was suggested by Woods *et al.*[60] and by Mathlouthi & Portmann,[13] based on calculations of the net atomic charges and the relative basicities of the hydroxyl groups[60] and IR-data rationalizations.[13] Interestingly, however, on the basis of intensity-time studies of the sweetness of glucose and fructose, that neither showed differences between α- and β-anomers

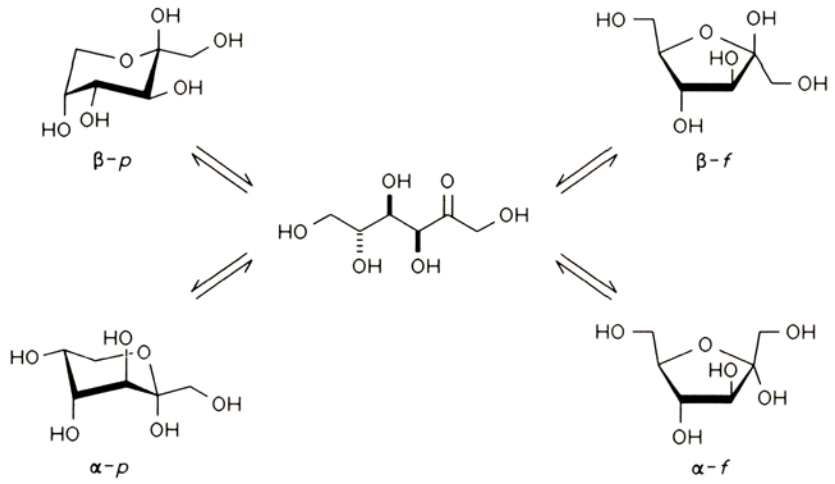

Fig. 8. Tautomeric forms of D-fructose (**2**). For an equilibrated aqueous solution at 25°C the composition is 73% β-*p*, 20% β-*f*, 5% α-*f*, and 2% α-*p* forms,[56,57] the acyclic *keto*-form is negligible.

nor in their apparent molar volumes, Birch *et al.*[61] arrived at an entirely different conclusion: the anomeric centre of D-fructose plays no direct role in the sweetness response, but rather the 3,4-diol system to which the AH—B glucophore is to be assigned (Fig. 9 (iii)).

For generation of the MEP and MLP profiles for β-D-fructopyranose, with which these assignments were to be probed, the relevant conformations of the hydroxymethyl group relative to the $^2C_5$-fixed pyranoid ring had to be determined. In the solid state, as evidenced by X-ray structural data,[54] the *gauche-gauche* (*gg*) arrangement† of the primary hydroxy group (A in Fig. 10) is realized. Undoubtedly, this *gg*-rotamer is one form relevant also in aqueous solution, with the minor modification though, that the weak intramolecular hydrogen bond circuit observed in the crystal lattice is disintegrated, since in water the hydroxyl groups can satisfy their hydrogen bond requirements by bonding with the solvent.

Semiempirical calculations of other conformations of **2** are encumbered with the fact that the minimum energy geometries generated represent the

†The conformation of the hydroxymethyl group is defined by two dihedral angles, the first referring to the $O_1—C_1—C_2—O_5$ torsion angle (*g* = gauche, *t* = trans), the second to $O_1—C_1—C_2—C_3$; the three staggered conformers are hence *gg*, *gt*, and *tg*.

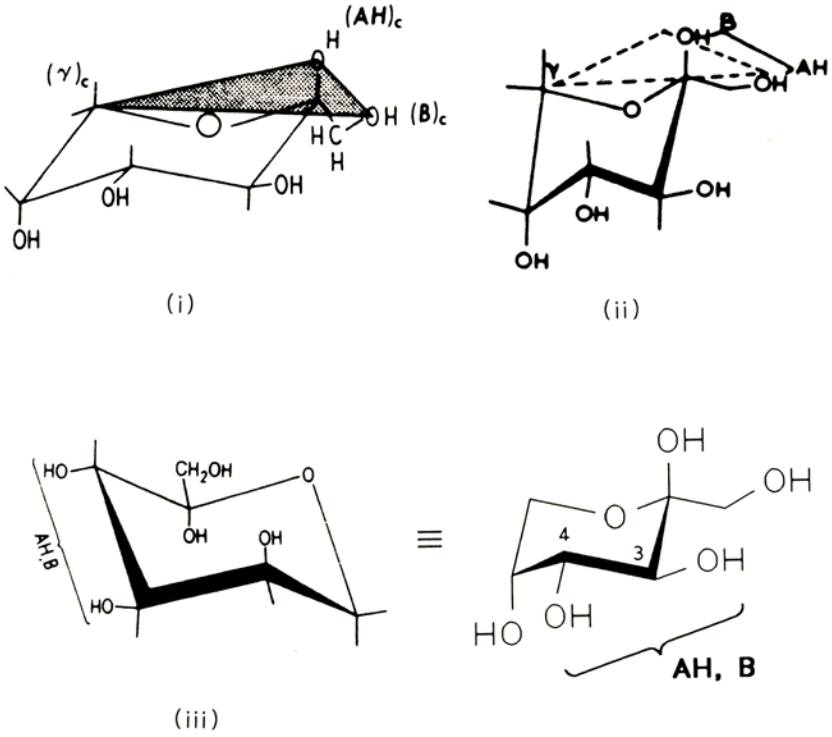

Fig. 9. Location of the tripartite AH—B—X glucophore in β-D-fructopyranose as suggested by Shallenberger[58] and Lindley & Birch[59] (i), by Woods *et al.*[60] and Mathlouthi & Portmann[13] (ii), and by Birch *et al.*[61] (iii).

state *in vacuo*, which may substantially be altered on solvation with water. This applies to the conformations emerging from very elaborate *ab initio* calculations[60,62] and AM 1-based semiempirical investigations,[63] as well as to those emanating from the more simple PIMM-88 force field methodology.[64] From the latter, the *tg*-rotamer C (Fig. 10) comes out to be the global minimum energy conformation, despite the steric constraints of the 1,3-diaxial-like arrangement of the 1-OH and 3-OH groups, which obviously are overcome (*in vacuo*) by the stabilizing effect of the intramolecular hydrogen bond 1-OH · · · O-3 (2·03 Å). This situation is most unlikely to prevail in water, particularly in view of recent molecular dynamics simulations for methyl β-D-glucopyranoside,[38] which convincingly proved the *in vacuo* minimum energy *tg*-form not to survive in water.

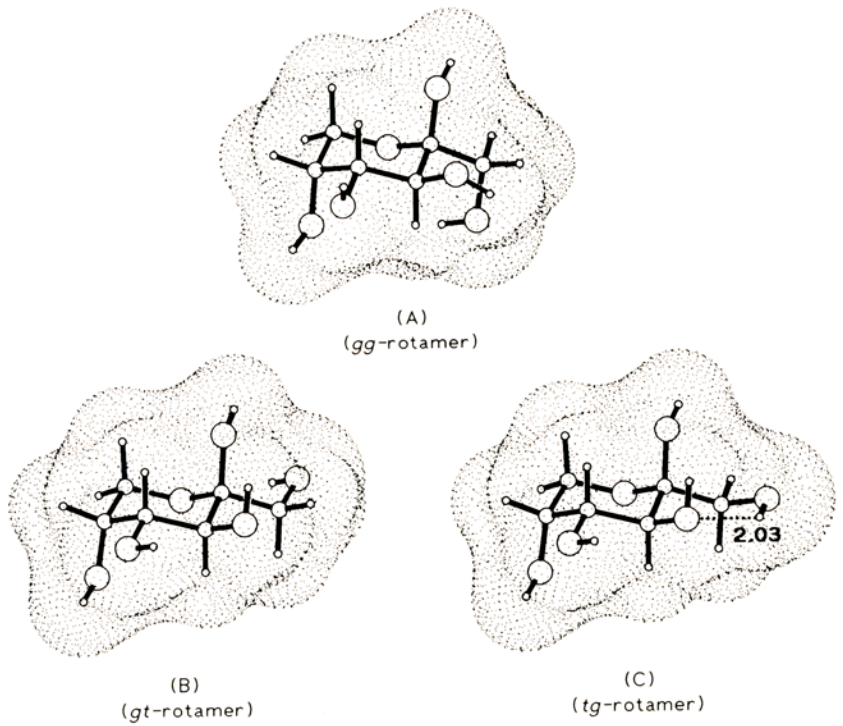

Fig. 10. The three staggered rotameric forms of the hydroxymethyl group in β-D-fructopyranose as derived from X-ray structural data[54] (A) and from force field calculations[64] (B and C), and their respective contact surfaces (in dotted form). The *tg*-rotamer (C), despite the unfavourable 1,3-diaxial-like interactions between the 1- and 3-OH group emerges as the lowest energy conformer, due to its stabilization by an intramolecular hydrogen bond 1-OH · · · O-3 (2·03 Å) *in vacuo*. Since this hydrogen bond will not survive solvation with water, the *tg*-rotamer is unlikely to be present in aqueous solutions.

This leaves the *gg*- and *gt*-rotamers of β-D-fructopyranose as the molecular conformations preferred in solution, and for which the contact surfaces (Fig. 10) and the MLP profiles were generated.[64] As is clearly evident from Plate 6, both forms have their most hydrophilic surface area (red) centred around the fructose-4-OH, whilst the hydrophobic (violet) part(s) are associated with either of the two methylene groups: in the *gg*-rotamer (left entries in Plate 6), the two methylene groups are connected with a 'hydrophobic band' that occupies half of the contact surface — as contrasted by the pattern of the *gt*-rotamer (right in Plate 6), where

the hydrophobic surface areas of the 1- and 6-CH_2 groups are separated. Accordingly, the X-part of the tripartite AH—B—X glucophore can easily be located: a region (rather than a specific position) reaching from the 6-CH_2 to the 1-CH_2, and, as such, being reminiscent of the hydrophobicity pattern of sucrose (Plate 2). Thus, the MLP-derived hydrophobic areas of β-D-fructopyranose appear to correlate — at least roughly — with the X-part assignments of Fig. 9, that invariably were placed at the 6-CH_2.

Location of the AH—B entity on the basis of the MLP profiles of Plate 6 — or the corresponding MEP patterns not depicted here — is seemingly difficult. Yet, the concentration of the most hydrophilic domains around the fructose-4-OH seems to point to that position for either being the B or AH part, i.e. to the 3,4-diol grouping to represent the AH—B couple. Thus, the MLP profiles obtained for the two fructose conformers likely to be prevalent in solution favours Birch's[61] proposition (Fig. 9 (iii)), which designates the 3-OH and 4-OH as the AH—B part, respectively. In this context, it is noteworthy, that Szarek *et al.*[62] found as a result of *ab initio* investigations of **2**, that O-4 in fructose exhibits enhanced basicity, while the secondary 4- and 3-OH protons seem to be relatively acidic, only being exceeded by the primary OH-group. These findings — in conjunction with the fact emerging from calculations of molecular electrostatic potentials[62] that 'the O-4 atom would be predicted to be the most attractive site for protonation'[62] — may be taken as a hint for the importance of the 4-OH group in respect to structure–sweetness relationships.

Considerations of the few relevant fructose analogues, whose sweetness characteristics are known, provides no solid evidence with which a clearcut decision between the putative AH—B-assignments of Fig. 9 could be made. That β-D-arabinose (**56**), 2-deoxy-fructose (**57**, 1,5-anhydro-D-mannitol), and the 2-*O*-methyl derivative **58** (methyl β-D-fructopyranoside) are considerably less sweet than the parent fructose[59] (Fig. 11) advocates the anomeric hydroxyl group to play a role in eliciting sweetness. On the other hand, the fact that sedoheptulosan **59** is as sweet as fructose[65] attests to the contrary.

The sweetness characteristics of analogues **60–63** tally with either of the conjectural assignments in Fig. 9: the 5-hydroxyl group can be replaced by hydrogen (→**60**) without losing sweetness,[66] and hence, as such is not an essential requirement for the sweetness sensation; however, its steric (axial) orientation is important since its configurational inversion to the 5-epimeric α-L-sorbopyranose (**61**) effects a substantial decrease in sweetness,[67] possibly by introducing a steric misfit upon interaction with the receptor.[66] Similarly, the intense sweetness of the 6-*thio* (**62**)[68] and 6-*carba*

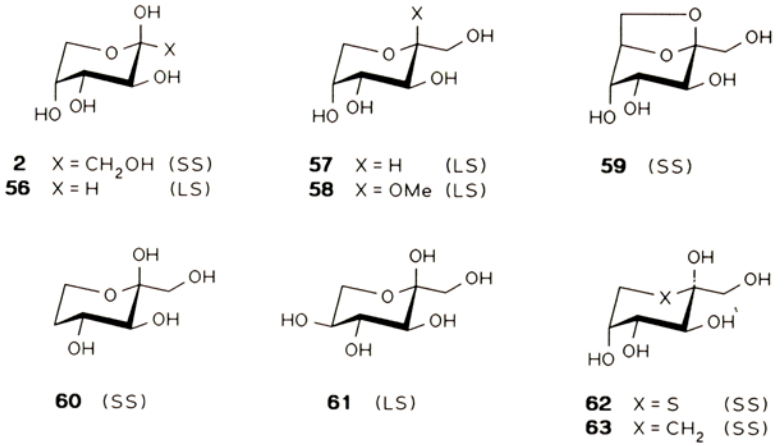

Fig. 11. Sweetness characteristics of analogues of β-D-fructopyranose (**2**). (SS: very sweet; LS: low sweetness.)

analogues (**63**)[69] of fructose (Fig. 11), although easily rationalized in terms of augmentation of the hydrophobic region within the 6-CH_2-1-CH_2 band, do not allow us to differentiate between a 1,2- or 3,4-diol grouping for the AH—B couple of the glucophore.

Although further evidence is required to settle this question unequivocally, as of now, we tend to attribute major significance to the MLP profiles obtained for the two fructose conformers likely to prevail in solution, and these (Plate 6) clearly favour Birch's proposal[61] (Fig. 9 (iii)), which places the AH—B couple of the glucophore into the 3,4-diol grouping of fructose. Moreover, when focussing on the essentials contained in the MLP pattern of the two fructose forms prevalent in solution (Plate 6), the basic feature emerges that hydrophobic and hydrophilic regions are located on opposite sides of the molecule — a situation quite similar to the one observed for sucrose (Plate 2). Thus, it may well be — and this receives fortification from the MLP profiles of a number of non-carbohydrate sweeteners (see below) — that the opposite-side-distribution of hydrophobic and hydrophilic regions, the latter being capable for hydrogen bonding with the receptor, is the principal structural feature for eliciting the sweetness response, rather than an AH—B—X 'sweetness triangle'.

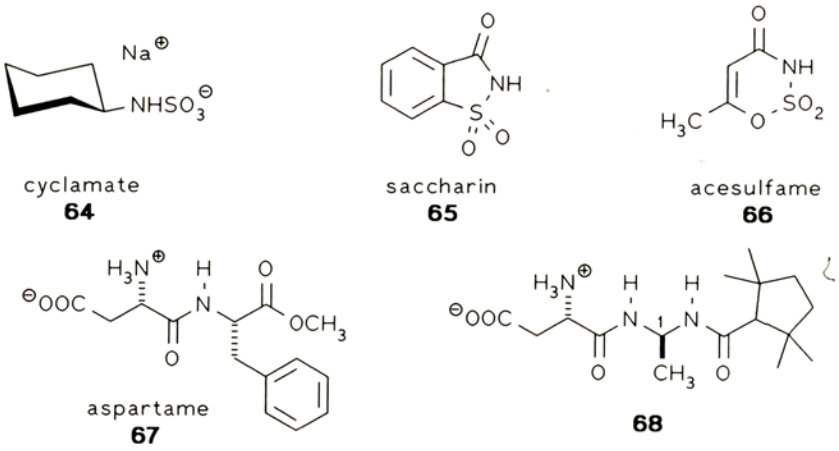

MLP PROFILES OF NON-CARBOHYDRATE, HIGH-POTENCY SWEETENERS

The AH—B—X glucophore concept has not only been applied to sugars, but has been appreciated as the unifying criterion for such structurally diverse sweet substances as amino acids and a series of non-carbohydrate sweeteners such as saccharin (**65**) and aspartame (**67**):[3] Serious reservations, however, must be advanced with respect to its general applicability, since it is known, for example, that the biologically active species of saccharin (**65**) and acesulfame (**66**) are the respective anions,[70] in which it is difficult to locate the AH entity. Furthermore, the AH—B—X concept assumes that all sweet molecules interact with the same receptor in the same, or in an at least very similar way — an assumption which is quite questionable. Recent evidence[71,72] either points to several types of sweet receptors, or to different kinds of activations within the same one, if indeed sugars and high-potency sweeteners really elicit the sweet response via the same taste receptors.

Despite these reservations it was obviously of interest to extend the molecular modelling techniques used above, to some representative non-carbohydrate sweeteners, as, for example, to compounds **64–68**. For this purpose, the solid state conformations were retrieved from the X-ray structural data available for saccharin (**65**),[73] acesulfame (**66**),[74] aspartame (**67**),[75] and the retro-inverso sweetener (**68**)[75] and used to calculate the respective contact surfaces (Figs. 12 and 13). In the case of cyclamate (**64**),

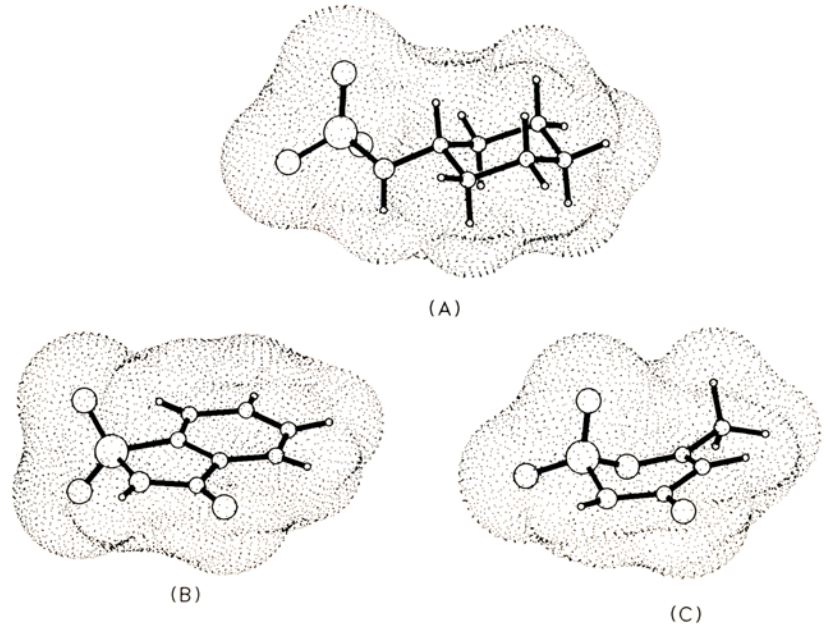

Fig. 12. Contact surface of cyclamate (**64**, A), saccharin (**65**, B), and acesulfame (**66**, C) in dotted contour form with stick-ball model insert. The conformation of **64** (A) was generated by force field calculations, those of **65** (B) and **66** (C) were modelled according to the X-ray structural data of the corresponding sodium or potassium salts.[73,74]

for which an X-ray structure is lacking, the conformation was generated by PIMM calculations.

As is clearly apparent from the contact surfaces of the three sulfamido sweeteners (Fig. 12), their overall molecular shapes are different, although the SO_2NH element is placed on the left side of each compound in Fig. 12 to accentuate their common structural as well as three-dimensional feature, undoubtedly involved in eliciting the sweet response.

However, when comparing their MLP profiles in Plate 7, the similarity of distribution of hydrophobic and hydrophilic regions is amazing; that the sulfamido grouping is the hydrophilic portion of the molecule was to be expected. That the differences between a cyclohexyl ring (in cyclamate), an aromatic moiety (as in saccharin) and an acetoacetyl residue fixed in the enol form (as in acesulfame) level off to yield hydrophobic areas closely

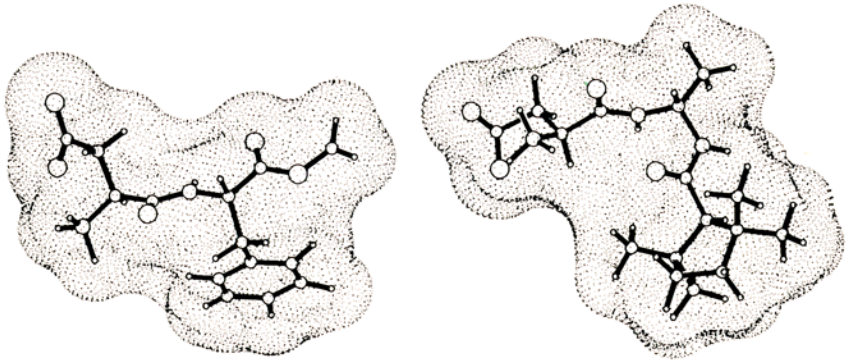

Fig. 13. Solid state conformation and contact surfaces, based on X-ray structural data[75,76] for A: the commercial dipeptide sweetener aspartame (**67**, 'Nutrasweet'®), and B: the intensely sweet *N*-*L*-aspartyl-*N*'-[(2,2,5,5-tetramethylcyclopentanyl)-carbonyl]-(*R*)-1,1,-diaminomethane (**68**), a retro-inverso dipeptide.

resembling each other — in the case of **65** and **66**, the two lower entries in Plate 7 are essentially identical — is most remarkable.

Another striking feature is that hydrophobic and hydrophilic portions of the molecules are on opposite sites, as in the case of sucrose and fructose (cf. above). Moreover, the very same distinct separation of hydrophilic and hydrophobic areas is observed for the dipeptide sweeteners **67** (aspartame) and **68**, which appear to be quite different in their solid state conformations (stick-ball model insert in Fig. 13), yet foreshadow a basic molecular shape similarity in their contact surfaces (Fig. 13, in dotted contours), which fully tallies with the respective MLP profiles of Plate 8: closely corresponding hydrophobic (violet) regions of such diverse elements as the aromatic ring of the phenylalanine portion of aspartame, and the sterically constrained tetramethylcyclopentyl group in **68**.

All of this sustains the notion, that the sweet receptor — be it the same for sucrose, fructose, and non-carbohydrate sweeteners or different ones — is quite flexible in adapting to the hydrophobic portion of sweet substances, i.e. to the X part (of the tripartite AH—B—X glucophore), which clearly is not a specific position of the molecule, but an entire region. If this hydrophobic area is the main factor governing the 'docking procedure' of the sweet substance, i.e. directing it to and locking it into the complementary 'hydrophobic cleft' of the receptor protein, it can well be

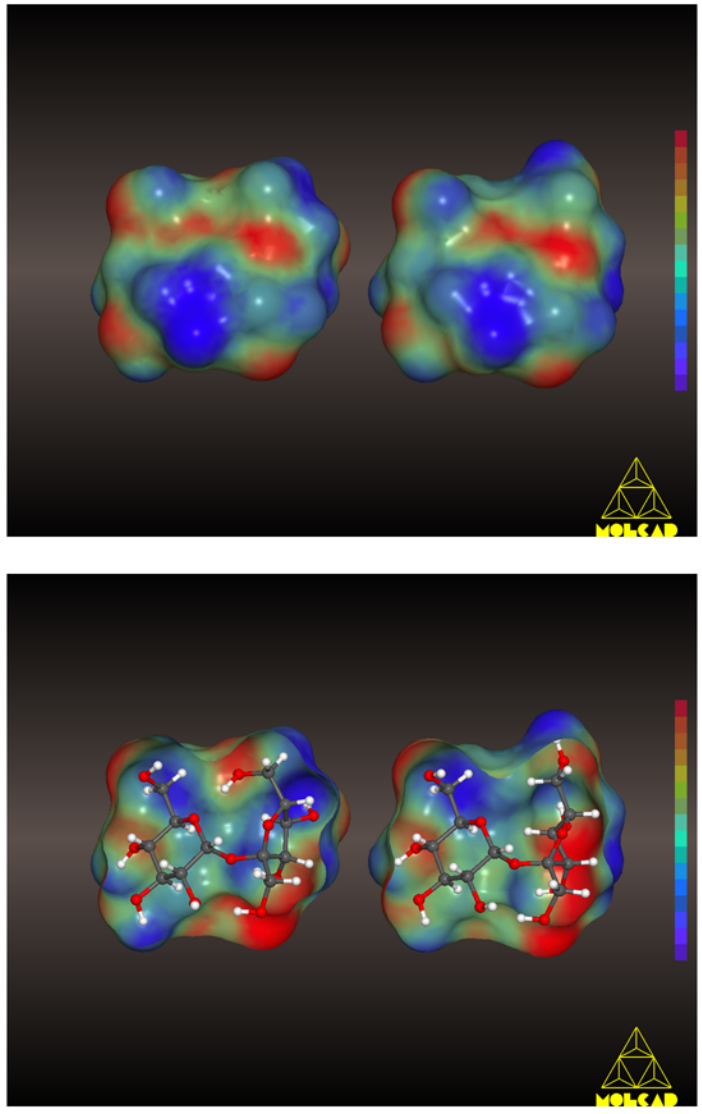

Plate 1. Molecular electrostatic potential (MEP) of sucrose in its conformation adopted in the crystal[15] (closed and opened form with ball-stick model insert on the left each), and its most probable 'solvated' form in solution (right each), represented on the respective contact surface in a 16-colour code, violet representing the positive maximum, i.e. the most electropositive and red the most electronegative portion of the molecule in relative terms.

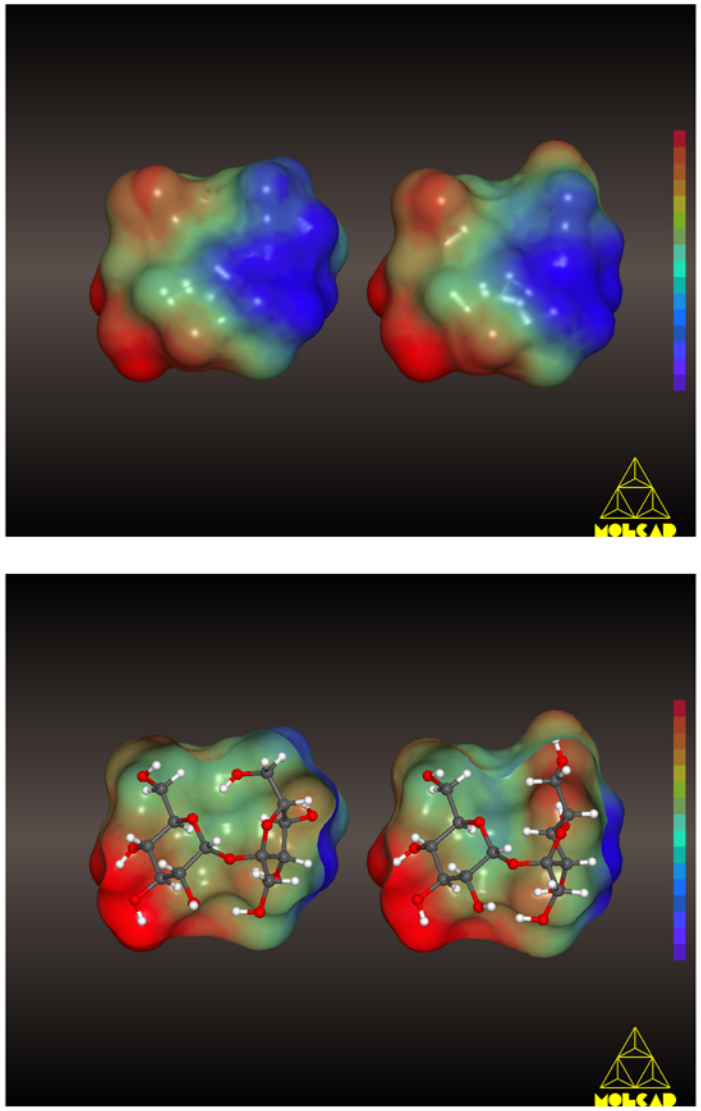

Plate 2. Molecular hydrophobicity potential (MLP) of sucrose as distributed over the contact surface in 16 colours ranging from violet (most hydrophobic) to red (most hydrophilic area): on the left side each, the MLP for the solid state conformation as derived from neutron diffraction data,[15] on the right the MLP for the conformation likely to prevail in solution. As is clearly apparent, the hydrophobic and hydrophilic regions are located on opposite sides of the molecules.

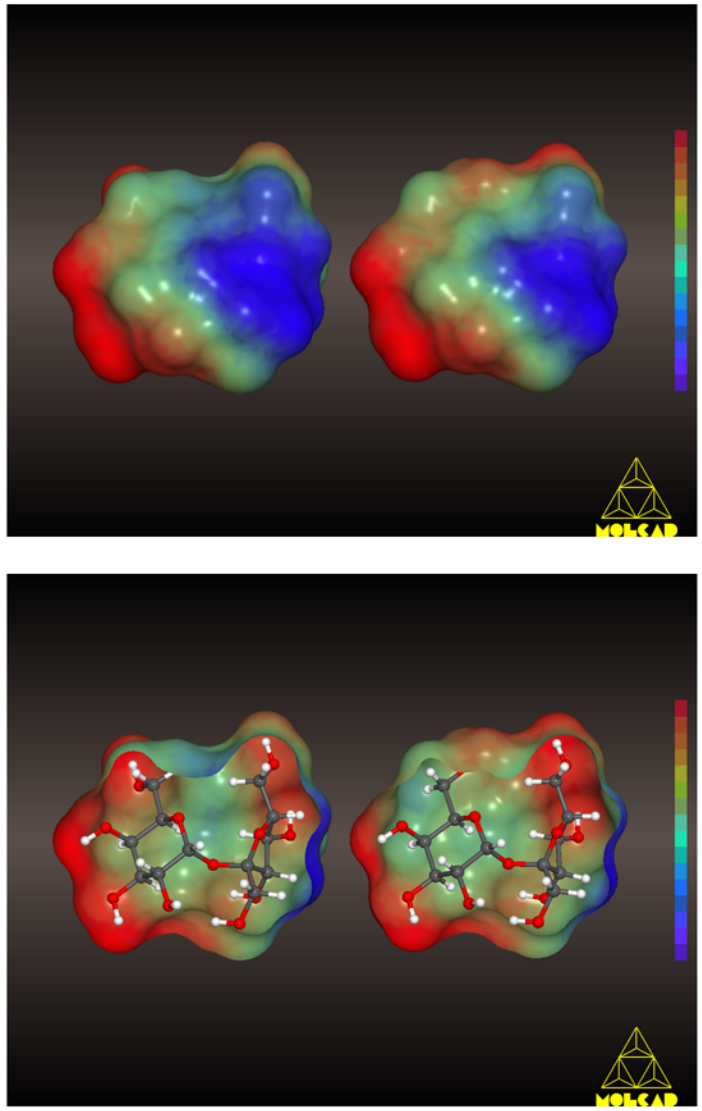

Plate 3. Hydrophobicity potential (MLP) profiles of the *tg*- (left) and *gt*-rotamers (right) of *galacto*-sucrose (**22**), corresponding to the forms C and D in Fig. 5.

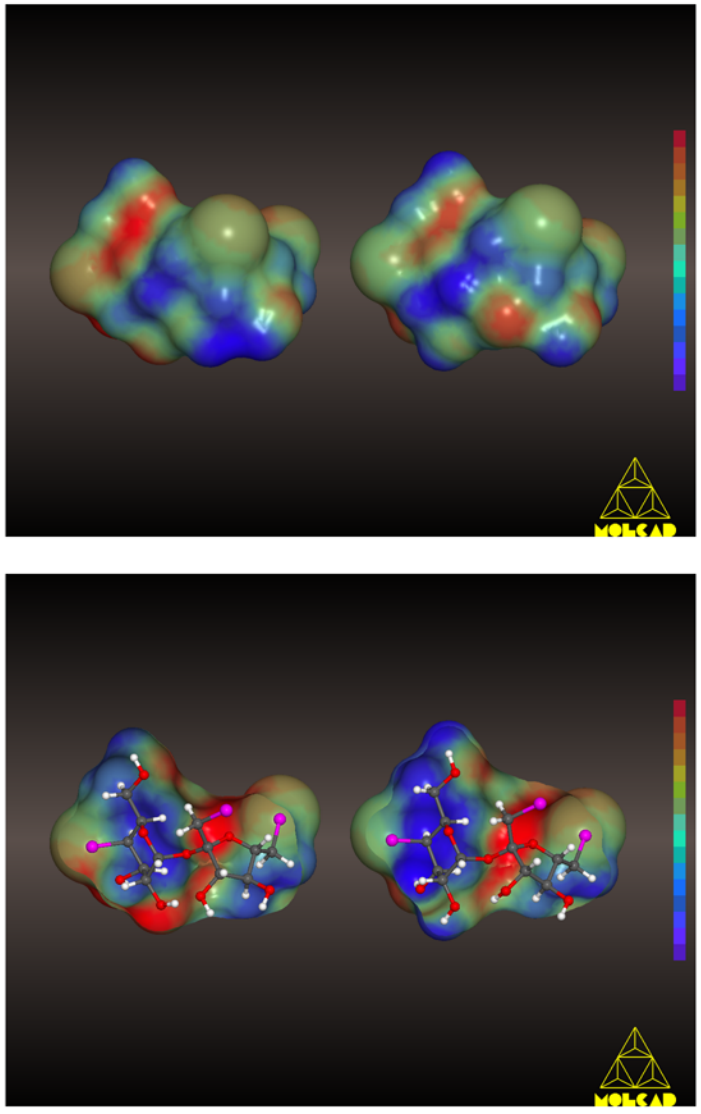

Plate 4. Molecular electrostatic potential (MEP) profile on the contact surface of sucralose (**3**) in the crystal[52] (left) and in the form generated by calculations (right), which, conceivably, has closer correspondence to the form prevalent in solution (violet: electropositive, red: electronegative).

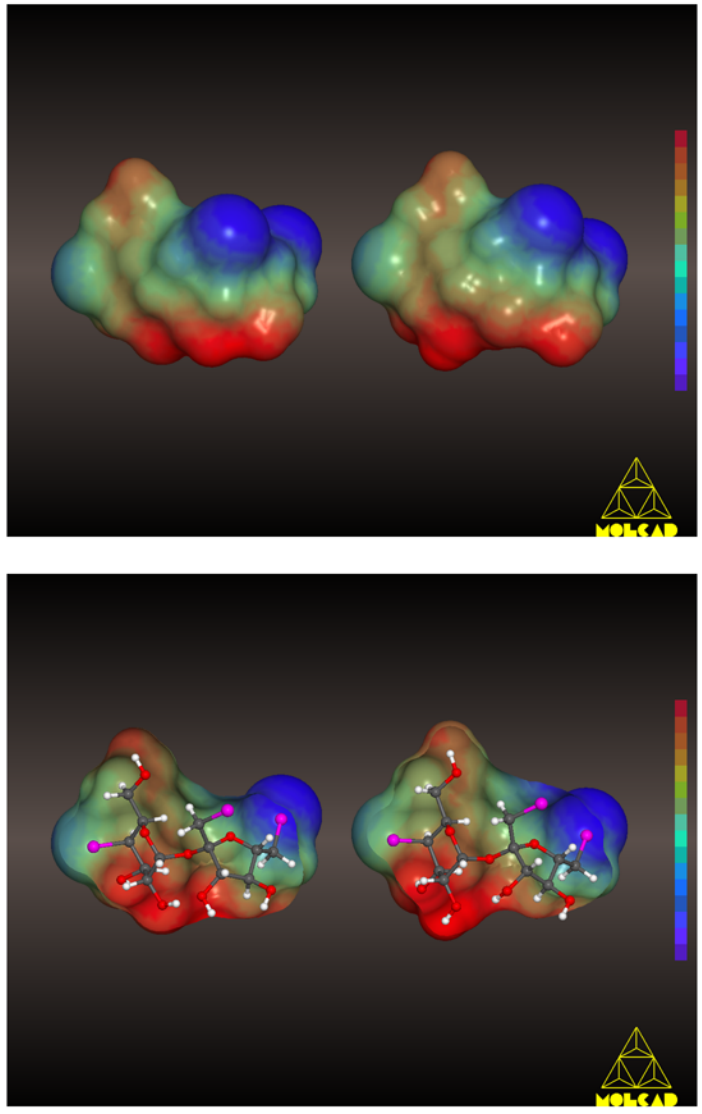

Plate 5. Molecular hydrophobicity potential (MLP) patterns of sucralose (**3**) in the solid state, X-ray structure[52] derived form (left), and the computer-simulated conformation (right). The reversal of the direction of the interresidue hydrogen bond from 2^{g}-OH $\cdots$ O-3^{f} (left) to 2^{g}-O $\cdots$ HO-3^{f} (right) results in a concentration of the hydrophilic area (red) around O-2^{g}.

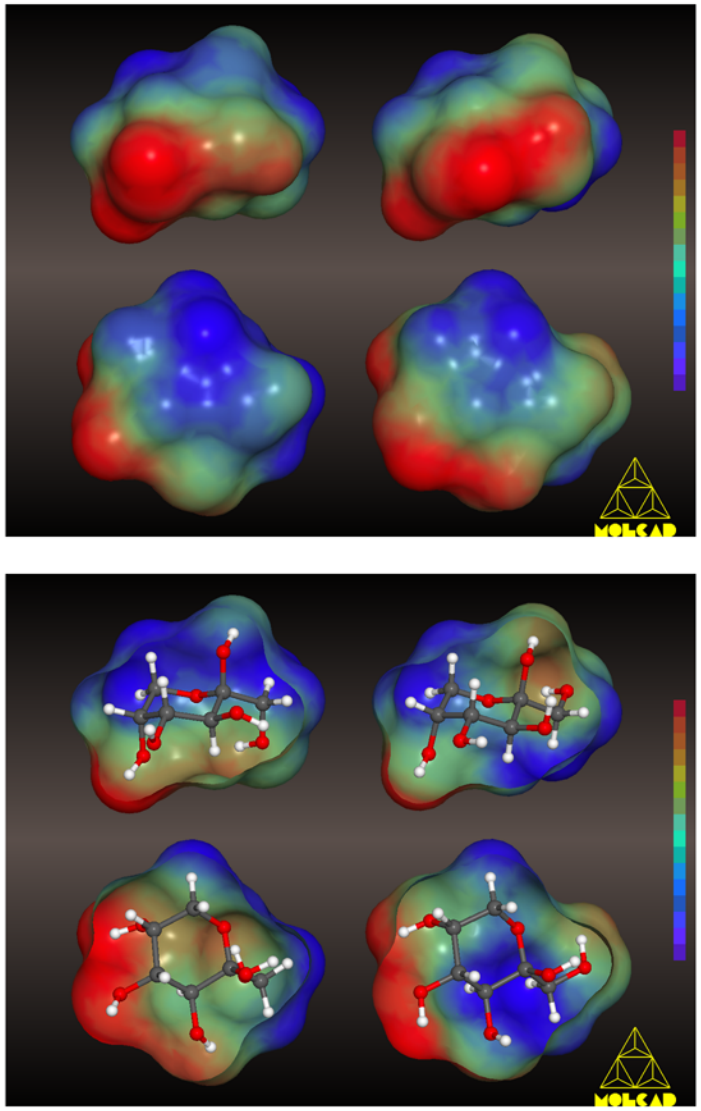

Plate 6. Molecular hydrophobicity potential (MLP) profiles for two conformers of β-D-fructopyranose (**2**), differing in the disposition of the hydroxymethyl group relative to the pyranoid ring: the *gg*-conformer is depicted on the left side each, the *gt*-form on the right. For each form, two representations were chosen, the upper corresponding in their orientations to those of Fig. 10 (B and C) respectively; the modellings depicted underneath were chosen in addition to better illustrate the opposite location of hydrophilic and hydrophobic regions.

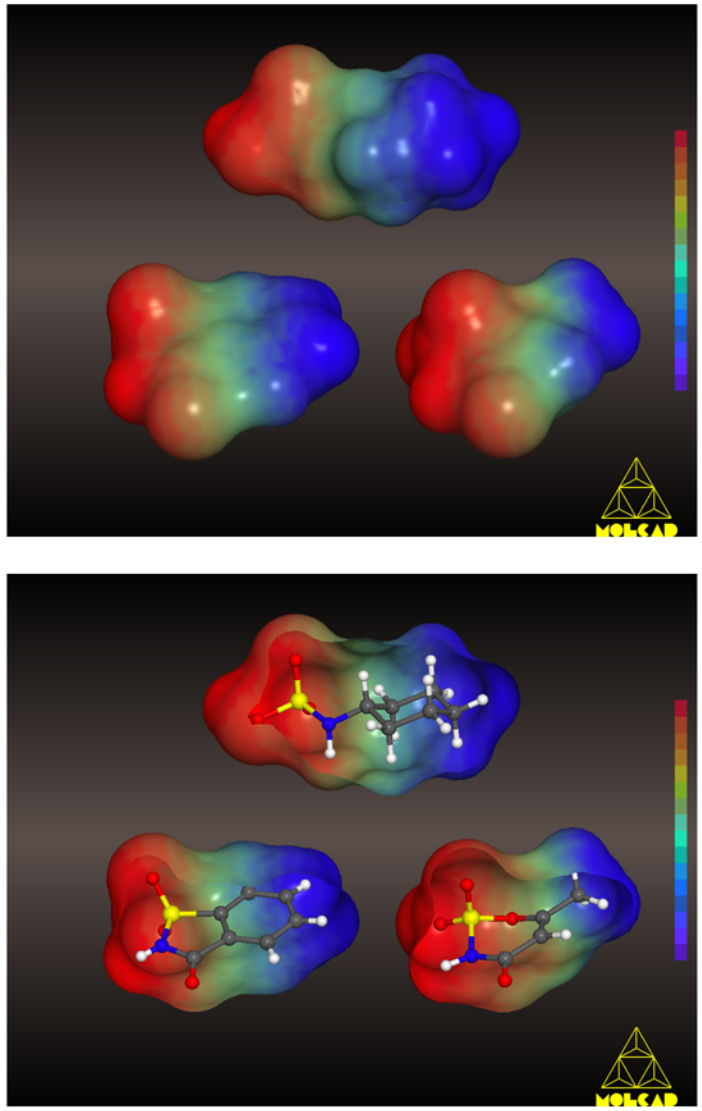

Plate 7. The molecular hydrophobicity potential (MLP) profiles in colour-coded representation (violet: hydrophobic, red: hydrophilic regions) of the sulfamide sweeteners cyclamate (**64**, upper middle), saccharin (**65**, lower left), and acesulfame (**66**, lower right) in closed and opened form; the MLPs are scaled separately to the range of the hydrophobicity potential calculated onto the respective contact surfaces (cf. Fig. 12).

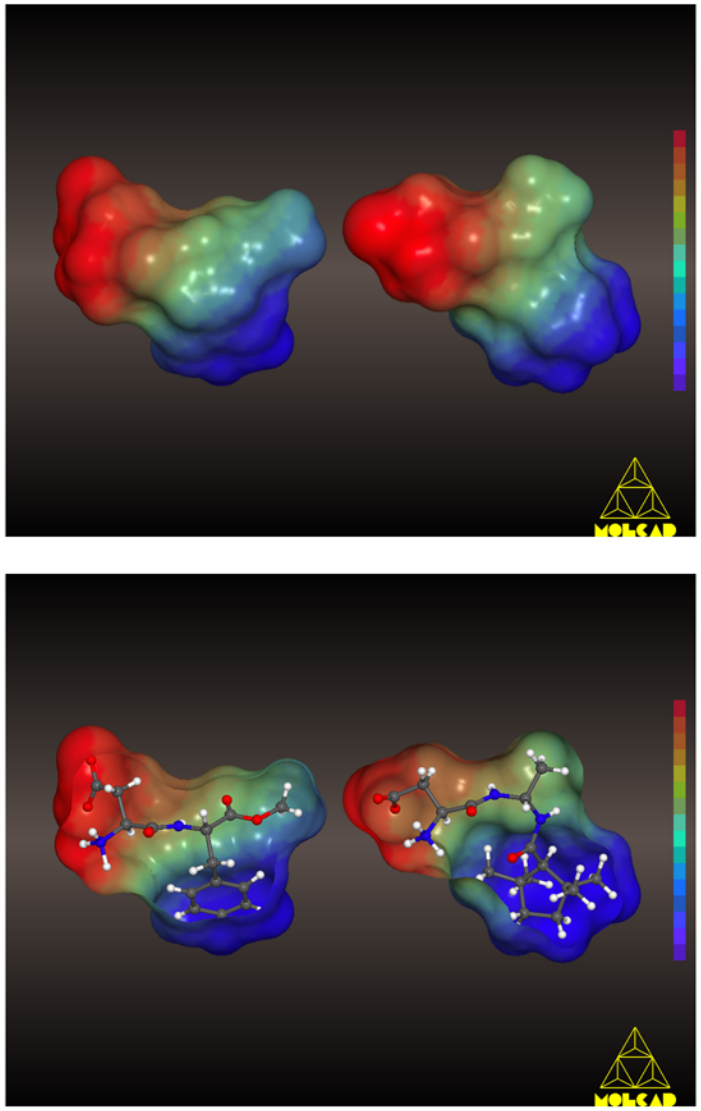

Plate 8. MLP profiles of the dipeptide sweeteners aspartame (**67**, left) and *N*-L-aspartyl-*N'*-[(2,2,5,5-tetramethylcyclopentanyl)-carbonyl]-(*R*)-1,1-diaminomethane (**68**, right) based on their crystal conformations.[75,76]

imagined that, thereby, the hydrophilic area of the molecule, situated on its opposite site, and likely to contain the AH—B portion of the Shallenberger–Kier tripartite AH—B—X glucophore, is brought into the appropriate position to elicit the sweet response via hydrogen bonding to a complementary receptor site AH—B couple.

In summary, much remains to be learned about the intricacies of the mechanism(s) involved in activation of sweet-sensitive cells, and direct solid evidence is urgently required. Nevertheless, the incorporation of the three-dimensional shape of sweet molecules, of their contact surfaces, and, particularly, inclusion of their MEP and MLP profiles into structure–sweetness considerations, has provided this field with a new dynamic vision, not only of the sweet molecule as such, but also of its complementary binding site. This revelation may lead, via computer-aided receptor modelling, to more realistic structure–sweetness concepts than those heretofore developed.

ACKNOWLEDGEMENTS

This work was supported by the Bundesministerium für Forschung und Technik (Grant No. 319257 A). We are grateful to Professor Dr. J. Brickmann, Institute of Physical Chemistry, Technische Hochschule of Darmstadt, for granting us access to his MOLCAD program and to the Silicon Graphics workstation.

REFERENCES

1. Studies on Ketoses, Part 6. — Part 5: Lichtenthaler, F.W. & Boettcher, A. (1993). In: *Nachwachsende Rohstoffe — Perspektiven für die Chemie*, Ed. M. Eggersdorfer, S. Warwel & G. Wolff, VCH Publishers, Weinheim/New York. (in press).
2. (a) Shallenberger, R.S. (1963). *J. Food Sci.*, **28**, 584–9.
   (b) Shallenberger, R.S. & Acree, T.E. (1967). *Nature*, **216**, 480–2; (1969). *J. Agric. Food Chem.*, **17**, 701–3.
3. Kier, L.B. (1972). *J. Pharm. Sci.*, **61**, 1394–7.
4. see Lee, C.K. (1987). *Adv. Carbohydr. Chem. Biochem.*, **45**, 199–351 (for a pertinent review).
5. (a) Lancet, D. & Ben-Arie, N. (1991). In: *Sweeteners: Discovery, Molecular Design, and Chemoreception*, Ed. D.E. Walter, F.T. Orthoefer & G.E. Dubois, ACS Symposium Series 450, Am. Chem. Soc., Washington, D.C., pp. 226–36.
   (b) Simon S.A. (1991). In: *Sweeteners: Discovery, Molecular Design, and Chemoreception*, Ed. D.E. Walter, F.T. Orthoefer & G.E. Dubois, ACS Symposium Series 450, Am. Chem. Soc., Washington, D.C., pp. 237–50.

6. Dubois, G.E., Walters, D.E. & Kellog, M.S. (1993). In: *Sweet-Taste Chemoreception*, Ed. M. Mathlouthi, J.A. Kanters & G.G. Birch, Elsevier Applied Science, London/New York (This monograph).
7. French, A.D. & Brady, J.W. (Eds.) (1990). *Computer Modelling of Carbohydrate Molecules*, ACS Symposium Series 430, Am. Chem. Soc., Washington, D.C.
8. Lichtenthaler, F.W., Immel, S. & Kreis, U. (1991). *Starch/Stärke*, **43**, 121–132; In: *Carbohydrates as Organic Raw Materials*, Ed. F.W. Lichtenthaler, VCH Publishers, Weinheim, New York, pp. 1–32.
9. Lichtenthaler, F.W. (1991). *Zuckerindustrie (Berlin)*, **116**, 701–12.
10. Hough, L. & Khan, R. (1989). In: *Progress in Sweeteners*, Ed. T.H. Grenby Elsevier Appl. Sci., London/New York, pp. 97–120.
11. James, C.E., Hough, L. & Khan, R. (1989). *Progr. Chem. Org. Nat. Prod.*, **55**, 117–84.
12. Hough, L. (1991). In: *Carbohydrates as Organic Raw Materials*, Ed. F.W. Lichtenthaler, VCH Publishers, Weinheim/New York, pp. 33–55.
13. Mathlouthi, M. & Portmann, M.O. (1990). *J. Mol. Struct.*, **237**, 327–38.
14. Shallenberger, R.S. (1964). *Agric. Sci. Rev.*, **2**, 11–20; see also Ref. 4, p. 260.
15. (a) Brown, G.M. & Levy, H.A. (1963). *Science*, **141**, 921–23.
(b) Brown, G.M. & Levy, H.A. (1973). *Acta Crystallogr., Sect. B*, **29**, 790–7.
(c) Hanson, J.C., Sieker, L.C. & Jensen, L.H. (1973). *Acta Crystallogr., Sect. B*, **29**, 797–808.
16. Bock, K. & Lemieux, U. (1982). *Carbohydr. Res.*, **100**, 63–74.
17. McCain, D.C. & Markley, J.L. (1986). *Carbohydr. Res.*, **152**, 73–80; *J. Am. Chem. Soc.*, **108**, 4259–64.
18. Christofides, J.C. & Davies, D.B. (1985). *J. Chem. Soc., Chem. Commun.*, 1533–4.
19. Davies, D.B. & Christofides, J.C. (1987). *Carbohydr. Res.*, **163**, 269–74.
20. (a) Tran, V.H. & Brady, J.W. (1990). *Biopolymers*, **29**, 961–76, 977–97.
(b) Tran, V.H. & Brady, J.W. (1990). In: *Computer Modeling of Carbohydrate Molecules*, Ed. A.D. French & J.W. Brady, ACS Symposium Series 430, Am. Chem. Soc., Washington, D.C., pp. 213–26.
21. Hervé du Penhoat, C., Imberty, A., Roques, N., Michon, V., Mentech, J., Descotes, G. & Pérez, S. (1991). *J. Am. Chem. Soc.*, **113**, 3720–7.
22. Lichtenthaler, F.W., Immel, S., Martin, D. & Müller, V. (1992). *Starch/Stärke*, **44**, (in press).
23. (a) Lindner, H.J. (1988). *PIMM-88, Closed Shell PI-SCF-LCAO-MO-Molecular Mechanics Program*, Technische Hochschule Darmstadt.
(b) Lindner, H.J. (1974). *Tetrahedron*, **30**, 1127–32.
(c) Smith, A.E. (1989). *Dissertation*, Technische Hochschule Darmstadt.
(d) Smith, A.E. & Lindner, H.J. (1991). *J. Comput. Aided Mol. Des.*, **5**, 235–62.
24. (a) Richards, F.M., (1977). *Annu. Rev. Biophys. Bioeng.*, **6**, 151–76.
(b) Connolly, M.L. (1983). *J. Appl. Cryst.*, **16**, 548–58; *Science*, **221**, 709–13.
25. Lee, B. & Richards, F.M. (1971). *J. Mol. Biol.*, **55**, 379–400.
26. Brickmann, J. & Waldherr-Teschner, M. (1991). *Informationstechnik* (Oldenburg Verlag, München), **33**, 83–90; Labo (Hoppenstedt Verlag, Darmstadt) **10** (1989) 7–14. The program MOLCAD (for *MOL*ecular *C*omputer *A*ided *D*esign) is an interactive, fast computer program for building and manipulating molecules and molecular systems. It is particularly suited to analyse and represent different physical molecular properties such as the electrostatic or hydrophobic potential on three-dimensional solid molecular surfaces, even of large molecules like proteins, zeolithes, and polymer MOLCAD runs on Silicon-Graphics 4D-workstations and can be licensed from the authors (Institut für Physikalische Chemie, Technische Hochschule Darmstadt, Petersenstraße 20, D-6100 Darmstadt, Germany).

27. Weiner, P.K., Langridge, R., Blaney, J.M., Schaefer, R. & Kollmann, P.A. (1982). *Proc. Natl. Acad. Sci. USA*, **79**, 3754–8.
28. (a) Stewart, J.J.P. (1990). *J. Comput. Aided Mol. Des.*, **4**, 1–105.
(b) Stewart, J.J.P. (1983). *Quantum Chem. Progr. Exchange Program* No. 455.
29. (a) Jeffrey, G.A. (1973). *Carbohydr. Res.*, **28**, 233–41.
(b) Jeffrey, G.A., Gress, M.E. & Takagi, S. (1977). *J. Am. Chem. Soc.*, **99**, 609–11.
(c) Tse, Y.-C. & Newton, M.D. (1977). *J. Am. Chem. Soc.*, **99**, 611–13.
(d) Jeffrey, G.A. & Takagi, S. (1978). *Acc. Chem. Res.*, **11**, 264–70.
(e) Jeffrey, G.A. & Lewis, L. (1978). *Carbohydr. Res.*, **60**, 179–82.
(f) Jeffrey, G.A. (1990). *Acta Crystallogr., Sect. B*, **46**, 89–103.
30. Wolf, P., Polligkeit, H. & Hamann, C.H. (1991). *Dechema-Monographie*, **124**, VCH Verlagsgesellschaft, 525–32.
31. (a) Ghose, A.K. & Crippen, G.M. (1986). *J. Comput. Chem.*, **7**, 565–77.
(b) Ghose, A.K., Pritchett, A. & Crippen, G.M. (1988). *J. Comput. Chem.*, **9**, 80–90.
(c) Furet, P., Sele, A. & Cohen, N.C. (1988). *J. Mol. Graphics*, **6**, 182–9.
(d) Fauchère, J.-L., Quarendon, P. & Kaetterer, L. (1988). *J. Mol. Graphics*, **6**, 202–6.
32. Ref. 11, p. 166.
33. Ref. 10, p. 108.
34. Lindley, M.G., Birch, G.G. & Khan, R. (1976). *J. Sci. Food Agric.*, **27**, 140–4.
35. Hough, L. (1989). *Int. Sugar J.*, **91**, 23–37.
36. Hough, L. & Khan, R. (1978). *Trends Biochem. Sci.*, **3**, 61–3.
37. Hough, L. & O'Brien, E. (1980). *Carbohydr. Res.*, **84**, 95–102.
38. Kroon-Batenburg, L.M.J. & Kroon, J. (1990). *Biopolymers*, **29**, 1243–48; and references cited therein.
39. Hough, L. & Phadnis, S.P. (1976). *Nature*, **263**, 800.
40. Hough, L. (1985). *Chem. Soc. Rev.*, **14**, 357–74.
41. Jenner, M.R. (1981). In: *Developments in Food Carbohydrates*, Vol. 2, Ed. C.K. Lee, Elsevier Applied Science, London, pp. 91–143.
42. Jenner, M.R. (1989). In: *Progress in Sweeteners*, Ed. T.H. Grenby, Elsevier Appl. Sci., London/New York, pp. 121–41.
43. Jenner, M.R. (1991). In: *Sweeteners: Discovery, Molecular Design, and Chemoreception*, Ed. D.E. Walter, F.T. Orthoefer & G.E. Dubois, ACS Symposium Series 450, Am. Chem. Soc., Washington, D.C., pp. 68–87.
44. Lee, C.K. (1987). *Carbohydr. Res.*, **162**, 53–63.
45. (a) Hough, L., Phadnis, S.P., Khan, R.A. & Jenner, M.R. (Tate & Lyle), *Brit. Pat.* 1.543.167 (1977). *Ger. Offen.* 2.700.917 (1977). [*Chem. Abstr.* **87** (1977) 202019 v].
(b) Hough, L., Phadnis, S.P., Khan, R.A. & Jenner, M.R. (Tate & Lyle), *Ger.*

Offen. 2.700.036 (1977) [*Chem. Abstr.*, **87** (1977) 202020 p].
(c) Khan, R.A., Hough, L. & Phadnis, S.P. (Tate & Lyle), *Brit. Pat.* 1.543.168 (1979) [*Chem. Abstr.*, **91** (1979) 193577 d].
46. Jackson, G., Jenner, M.R., Khan, R.A., Lee, C.K., Mufti, K.S., Patel, G.D. & Rathbone, E.B. (Tate & Lyle), *Brit. Pat.* 2.104.063 (1982), *Eur. Pat. Appl.* EP 73.093 (1983) [*Chem. Abstr.*, **99** (1983) 54127 j].
47. (a) Lee, C.K. (Tate & Lyle), *Brit. Pat.* 2.088.855 (1982), *Eur. Pat. Appl.* EP 50.952 (1982) [*Chem. Abstr.*, **97** (1982) 145225 q].
(b) Lee, C.K. (Tate & Lyle), *US Pat.* 4.405.654 (1983) [*Chem. Abstr.*, **100** (1984) 33495 b].
48. Khan, R.A., Mufti, K.S. & Patel, G.D. (Tate & Lyle), *Brit. Pat.* 2.127.806, *Eur. Pat. Appl.* EP 103.479 (1984) [*Chem. Abstr.*, **101** (1984) 23887 n].
49. (a) Jackson, G., Jenner, M.R. & Khan, R.A. (Tate & Lyle), *Brit. Pat.* 2.101.989 (1982), *Eur. Pat. Appl.* EP 67.535 (1982) [*Chem. Abstr.*, **98** (1983) 161107 d].
50. (a) Khan, R.A. & Jenner, M.R. (Tate & Lyle), *Brit. Pat.* 2.037.561 (1980), *Eur. Pat. Appl.* EP 10.409 (1980) [*Chem. Abstr.*, **93** (1980) 130944 s].
(b) Khan, R.A. & Jenner, M.R. (Tate & Lyle), *Brit. Pat.* 2.036.007 A (1980). *Eur. Pat. Appl.* EP 10.410 (1980) [*Chem. Abstr.*, **93** (1980) 150590 b].
51. Reicherzer, J. (1991). *Die Zeit (München)*, No. 40 (26. Sept.), 31.
52. (a) Jenner, M.R. & Waite, D. (Tate & Lyle PLC), *Brit. Pat.* 2.065.646 (1980), *Eur. Pat. Appl.* EP 30.804 (1981) [*Chem. Abstr.*, **95** (1981) 169699 g].
(b) Kanters, J.A., Scherrenberg, R.L., Leeflang, B.R., Kroon, J. & Mathlouthi, M. (1988). *Carbohydr. Res.*, **180**, 175–82.
53. Christofides, J.C., Davies, D.B., Martin, J.A. & Rathbone, E.B. (1986). *J. Am. Chem. Soc.*, **108**, 5738–43.
54. (a) Kanters, J.A., Roelofsen, G., Alblas, B.P. & Meinders, I. (1977). *Acta Crystallogr., Sect. B*, **33**, 665–72.
(b) Takagi, S. & Jeffrey, G.A. (1977). *Acta Crystallogr., Sect. B*, **33**, 3510–15.
55. Shallenberger, R.S. & Acree, T.E. (1971). In: *Handbook of Sensory Physiology IV; Chemical Senses, Part 2 — Taste*, Springer Verlag, Berlin, pp. 221–77.
56. Schneider, B., Lichtenthaler, F.W., Steinle, G. & Schiweck, H. (1985). *Liebigs Ann. Chem.*, 2443–53.
57. Lichtenthaler, F.W. & Rönninger, S. (1990). *J. Chem. Soc., Perkin Trans.*, **2**, 1489–97.
58. (a) Shallenberger, R.S., Acree, T.E. & Guild, W.E. (1965). *J. Food Sci.*, **30**, 560–3.
(b) Shallenberger, R.S. & Acree, T.E. (1967). *Nature*, **216**, 480–2.
(c) Shallenberger, R.S. & Lindley, M.G. (1977). *Food Chem.*, **2**, 145–53.
(d) Shallenberger, R.S. (1978). *Pure Appl. Chem.*, **50**, 1409–19.
59. Lindley, M.G. & Birch, G.G. (1975). *J. Sci. Food Agric.*, **26**, 117–24.
60. Woods, R.J., Smith, V.H., Jr., Szarek, W.A. & Farazdel, A. (1987). *J. Chem. Soc., Chem. Commun.*, 937–9.
61. Birch, G.G., Shamil, S. & Shepherd, Z. (1986). *Experientia*, **42**, 1232–4.
62. Szarek, W.A., Korppi-Tommola, S.-L., Martin, O.R. & Smith, V.H., Jr. (1984). *Can. J. Chem.*, **62**, 1506–11.
63. Woods, R.J., Szarek, W.A. & Smith, V.H., Jr. (1990). *J. Am. Chem. Soc.*, **112**, 4732–41.

64. Immel. S. & Lichtenthaler, F.W. (1992). Unpublished data.
65. Lee, C.K. & Birch, G.G. (1976). *J. Pharm. Sci.*, **65**, 1222–5.
66. Martin, O.R., Korppi-Tommola, S.-L. & Szarek, W.A. (1982). *Can. J. Chem.*, **60**, 1857–62.
67. Tsuzuki, T. & Yamazaki, J. (1953). *Biochem. Z.*, **323**, 525–31; (1953). *J. Chem. Soc. Jpn.*, **74**, 596–601.
68. Lindley, M.G., Shallenberger, R.S. & Whistler, R.L. (1976). *J. Food Sci.*, **41**, 575–7.
69. (a) Suami, T., Ogawa, S., Takata, M., Yasuda, K., Suga, A., Takei, K. & Uematsu, Y. (1985). *Chem. Lett.*, 719–22.
(b) Suami, T. (1987). *Pure Appl. Chem.*, **59**, 1509–20.
70. Janikovich, W. (1982). *J. Neurosci.*, **2**, 49.
71. Faurion, A., Saito, S. & Macleod, P. (1980). *Chem. Senses*, **5**, 107–21; Faurion, A. (1987). *Progress in Sensory Physiology*, Springer-Verlag Berlin/Heidelberg, pp. 130–201.
72. Dubois, G.E., Walters, D.E., Schiffmann, S.S., Warwick, Z.S., Booth, B.J., Pecore, S.D., Gibes, K., Carr, B.T. & Brands, L.M. (1991). In: *Sweeteners: Discovery, Molecular Design, and Chemoreception*, Ed. D.E. Walter, F.T. Orthoefer & G.E. Dubois, ACS Symposium Series 450, Am. Chem. Soc., Washington, D.C., pp. 261–76.
73. Bart, J.C.J. (1968). *J. Chem. Soc., B*, 376–82; Okaya, Y. (1969). *Acta Crystallogr., Sect. B*, **25**, 2257–63; Jovanovski, G. & Kamenar, B. (1982). *Cryst. Struct. Comm.*, **11**, 247.
74. Paulus, E.F. (1975). *Acta Crystallogr., Sect. B*, **31**, 1191–3.
75. Hatada, M., Jancarik, J., Graves, B. & Kim, S.-H. (1985). *J. Am. Chem. Soc.*, **107**, 4279–82.
76. Benedetti, E., DiBlasio, B., Pavone, V., Pedone, C., Fuller, W.D., Mierke, D.F. & Goodman, M. (1990). *J. Am. Chem. Soc.*, **112**, 8909–12.